Limited population structure but signals of recent selection in introduced African Fig Fly *(Zaprionus indianus*) in North America

Priscilla A. Erickson[1]*, Alexandra Stellwagen[1], Alyssa Bangerter[2], Ansleigh Gunter[1], Nikolaos T. Polizos[3], and Alan O. Bergland[2]

1. University of Richmond, Richmond, Virginia
2. University of Virginia, Charlottesville, Virginia
3. University of Miami, Coral Gables, Florida

**Corresponding author; perickso@richmond.edu*

Running title

Genomics of invasive *Zaprionus indianus*

Abstract

Invasive species have devastating consequences for human health, food security, and the environment. Many invasive species adapt to new ecological niches following invasion, but little is known about the early steps of adaptation. Here we examine population genomics of a recently introduced drosophilid in North America, the African Fig Fly, *Zaprionus indianus*. This species is likely intolerant of subfreezing temperatures and recolonizes temperate environments yearly. We generated a new chromosome-level genome assembly for *Z. indianus*. Using resequencing of over 200 North American individuals collected over four years in temperate Virginia, plus a single collection from subtropical Florida, we tested for signatures of population structure and adaptation within invasive populations. We show founding populations are sometimes small and contain close genetic relatives, yet temporal population structure and differentiation of populations is mostly absent across North America. However, we identify two haplotypes that are differentiated between African and invasive populations and show signatures of selective sweeps. Both haplotypes contain genes in the cytochrome P450 pathway, indicating these sweeps may be related to pesticide resistance. X chromosome evolution in invasive populations is strikingly different from the autosomes, and a haplotype on the X chromosome that is highly differentiated between Virginia and Florida populations is a candidate for temperate adaptation. These results show that despite limited population structure, populations may rapidly evolve genetic differences early in an invasion. Further uncovering how these genomic regions influence invasive potential and success in new environments will advance our understanding of how organisms evolve in changing environments.

Article Summary

Invasive species (organisms that have been moved outside their natural range by human activities) can cause problems for both humans and the environment. We studied the genomes

of over 200 individuals of a newly invasive fruit fly in North America, the African Fig Fly. We found genetic evidence that these recently introduced flies may be evolving in their new environments, which could make them stronger competitors and more likely to become pests.

Introduction

Understanding how species expand and adapt to new environments in an era of changing land use, environmental changes, and global commerce is central to controlling the spread of disease (Altizer et al. 2013; Hoberg and Brooks 2015), to maintaining crop security (Oerke 2006; Sutherst et al. 2011) and to preserving biodiversity (Bellard et al. 2012). Many organisms are moving to new, previously unoccupied ranges at rates that continue to accelerate (Ricciardi 2007; Seebens et al. 2015; Seebens et al. 2017; Platts et al. 2019; Sardain et al. 2019) due to changing environmental conditions, habitat alteration, and anthropogenic introductions. Genetic adaptation to new environments may allow some vulnerable organisms to survive in new habitats but may also permit potentially harmful organisms to expand even further (Clements and Ditommaso 2011). The past two decades have produced a wealth of studies characterizing the genetic and genomic basis of adaptation in a variety of organisms, from experimental populations of microbes (Good et al. 2017; Nguyen Ba et al. 2019; Johnson et al. 2021) to natural populations of eukaryotes (Hancock et al. 2011; Jones et al. 2018; Barrett et al. 2019; Lovell et al. 2021 Jan 27; Schluter et al. 2021). Recent and ongoing invasions offer the opportunity to study rapid evolution and adaptation to new environments in nearly real-time (Koch et al. 2020; Pélissié et al. 2022; Parvizi et al. 2023; Soudi et al. 2023). Recently, genomics has helped trace the history and sources of many well-known invasions (Pélissié et al. 2022; Picq et al. 2023) and shown that genetic divergence and even local adaptation are common in invasive populations that have been established for decades or even centuries (Ma et al. 2020; Stuart et al. 2021; Li et al. 2023). However, much remains unknown about the role that evolution plays in allowing invasive organisms to colonize and thrive in new environments. A better understanding of adaptive pathways in invasion may assist in predicting the success of invasions and controlling their outcomes.

The African Fig Fly, *Zaprionus indianus*, serves as a unique model to study how invasion history and local environment influence patterns of genetic variation. The ongoing, recurrent invasion of *Z. indianus* in North America offers a premier opportunity to study the possibility of rapid genetic changes following invasion. The *Zaprionus* genus arose in Africa but *Z. indianus* was first described in India in 1970 (Gupta 1970), where it has adapted to a range of environments (da Mata et al. 2010). It is one of the most ecologically diverse drosophilids in Africa; its ability to utilize up to 80 different food sources (Yassin and David 2010) and its generation time of as few as ~13 days (Nava et al. 2007) likely fueled its spread around the world. In 1999, it was first detected in Brazil (Vilela 1999), where it subsequently spread and caused major damage to fig and berry crops as well as native fruit species (Leão and Tldon 2004; Oliveira et al. 2013; Roque et al. 2017; Zanuncio-Junior et al. 2018; Allori Stazzonelli et al. 2023). It was later found in Mexico and Central America in 2002-2003 (Markow et al. 2014) and eventually Florida, USA in 2005 (Linde et al. 2006). In 2011-2012, its range expanded

northwards in eastern North America (Joshi et al. 2014; Timmeren and Isaacs 2014; Pfeiffer et al. 2019) and eventually reached as far north as Ontario, Canada (Renkema et al. 2013) and Minnesota, USA (Holle et al. 2018). It has also recently been found in the Middle East, Europe, and Hawaii (Parchami-Araghi et al. 2015; Kremmer et al. 2017; Willbrand et al. 2018), suggesting that the invasion is ongoing. *Z. indianus* can damage fig and berry crops (Pfeiffer et al. 2019; Allori Stazzonelli et al. 2023), increasing concerns about its pest potential in its expanding range.

Despite its global success, *Z. indianus* males are sterile below 15 °C, making cold temperatures a limiting factor to their success (Araripe et al. 2004). Within the temperate environment of Virginia, the species exhibits strong seasonal fluctuations in abundance (Rakes et al. 2023). First detection in Virginia is usually in June or July, weeks after the appearance of other overwintering drosophilids, and population sizes climb dramatically through the late summer and early fall, when it often dominates the drosophilid community in temperate orchards. Typically, the peak in early to mid-September is followed by a dip in abundance and then a second peak in October, suggesting a seasonal component to reproduction or fluctuations in factors influencing *Z. indianus'* relative fitness. However, despite its early post-colonization success, it does not appear to survive temperate winters; *Z. indianus* populations became undetectable in Virginia by early December (Rakes et al. 2023). *Z. indianus* were not collected during regular winter sampling in Memphis, Tennessee (Kohlmeier and Kohlmeier 2025), and they were collected in lower numbers during the winter in northern Florida relative to central Florida (Renkema et al. 2018), suggesting that even mild winters (only 8 nights below 0° C) can substantially reduce their numbers. In locations in Minnesota, Kansas, and the northeastern US, *Z. indianus* has been detected one year and then not the next, suggesting that the populations may be extirpated by cold and re-introduced by stochastic dispersal processes (Holle et al. 2018; Gleason et al. 2019; Rakes et al. 2023). While conclusive data are still lacking, these results collectively suggest *Z. indianus* likely repeatedly invades temperate environments each year from warmer refugia. Reinvasion offers an opportunity to recurrently study the genetic impacts of invasion and the potential for post-colonization adaptation across multiple years of sampling.

Genetic *s*tudies *of Z. indianus* are limited but provide important context to understand its worldwide invasion. The invasion of North America likely resulted from separate founding events on the East and West coasts (Commar et al. 2012). Comeault et al. (2020) showed that North American populations are genetically distinct from those from Africa. Invasive populations of *Z. indianus* have an approximately 30% reduction in genetic diversity relative to ancestral African populations (Comeault et al. 2020), though invasive populations of *Z. indianus* maintain levels of genetic diversity that are often higher than those of non-invasive congeners. Despite the loss of diversity, *Z. indianus* is extremely successful in temperate habitats (Rakes et al. 2023). Further studies demonstrated that genetically distinct populations from eastern and western Africa likely admixed prior to a single colonization of the Americas (Comeault et al. 2021). How the high degree of genetic diversity in invasive populations

129 influences the potential for ongoing evolution in North America, which is in a critical early stage
130 of invasion, remains understudied.
131
132 Here, we assembled and annotated a chromosome-level genome assembly for *Z.*
133 *indianus* and used the newly improved genome to answer several questions with the whole
134 genome sequences of over 200 North American flies collected from three locations over four
135 years. First, do recolonizing North American *Z. indianus* populations demonstrate spatial or
136 temporal population structure and if so, do specific regions of the genome have an outsized
137 contribution to population structure? Second, is the invasion and recolonization history
138 recapitulated in population genetic data? And third, do temperate populations show signatures
139 of selection relative to native and tropical invasive populations?
140
141 **Materials and Methods**
142
143 *Hi-C based genome scaffolding*
144
145 An inbred line was generated from flies originally captured from Carter Mountain Orchard, VA
146 (37.9913° N, 78.4721° W) in 2019. Wild caught flies were reared in the lab for approximately
147 one year prior to initiating isofemale lines. The offspring of the isofemale lines were propagated
148 through 10 rounds of full-sib mating. The resulting lines were then passaged for approximately
149 one additional year in the lab and the most vigorous remaining line ("24.2") was chosen for
150 sequencing.
151
152 Third instar larvae from a single inbred line were snap frozen in liquid nitrogen and sent
153 to Dovetail corporation (now Cantata Bio, Scotts Valley, CA) for chromatin extraction, Hi-C
154 sequencing and genome scaffolding. Briefly, chromatin was fixed in place with formaldehyde in
155 the nucleus and then extracted. Fixed chromatin was digested with DNase I, chromatin ends
156 were repaired and ligated to a biotinylated bridge adapter followed by proximity ligation of
157 adapter containing ends. After proximity ligation, crosslinks were reversed and the DNA
158 purified. Purified DNA was treated to remove biotin that was not internal to ligated fragments.
159 Sequencing libraries were generated using NEBNext Ultra enzymes and Illumina-compatible
160 adapters. Biotin-containing fragments were isolated using streptavidin beads before PCR
161 enrichment of each library. The library was sequenced on an Illumina HiSeqX platform to
162 produce approximately 30x sequence coverage.
163
164 The input *de novo* assembly was the *Z. indianus* "RCR04" PacBio assembly (assembly
165 # ASM1890459v1) from Kim et al. (2021). This assembly and Dovetail OmniC library reads
166 were used as input data for *HiRise*, a software pipeline designed specifically for using
167 proximity ligation data to scaffold genome assemblies (Putnam et al. 2016). Dovetail OmniC
168 library sequences were aligned to the draft input assembly using *bwa* (Li and Durbin 2009).
169 The separations of Dovetail OmniC read pairs mapped within draft scaffolds were analyzed by
170 *HiRise* to produce a likelihood model for genomic distance between read pairs, and the model

171 was used to identify and break putative misjoins, to score prospective joins, and make joins
172 above a threshold. See Figure S1 for link density histogram of scaffolding data.
173
174 *Annotation*
175
176 Repeat families found in the genome assemblies of *Z. indianus* were identified de novo and
177 classified using the software package *RepeatModeler* v. 2.0.1 (Flynn et al. 2020).
178 *RepeatModeler* depends on the programs *RECON* v. 1.08 (Bao and Eddy 2002) and
179 *RepeatScout* v. 1.0.6 (Price et al. 2005) for the de novo identification of repeats within the
180 genome. The custom repeat library obtained from *RepeatModeler* was used to discover,
181 identify and mask the repeats in the assembly file using *RepeatMasker* v. 4.1.0 (Smit et al.
182 2015).
183
184 RNA sequencing was conducted on three replicates of 3rd instar larva and three
185 replicates of mixed stage pupa that were snap frozen in liquid nitrogen. RNA extraction and
186 sequencing was performed by GeneWiz (South Plainfield, NJ). New larval and pupal RNAseq
187 reads were combined with adult RNA sequencing from Comeault et al. (2020) for annotation.
188 Coding sequences from *D. grimshawi, D. melanogaster*, *D. pseudoobscura*, *D. virilis*, *Z.*
189 *africanus*, *Z. indianus*, *Z. tsacasi* and *Z. tuberculatus* (Kim et al. 2021) were used to train the
190 initial *ab initio* model for *Z. indianus* using the *AUGUSTUS* software v. 2.5.5 (Keller et al.
191 2011). Six rounds of prediction optimization were done with the software package provided by
192 *AUGUSTUS*. The same coding sequences were also used to train a separate *ab initio* model
193 for *Z. indianus* using *SNAP* (version 2006-07-28) (Korf 2004). RNAseq reads were mapped
194 onto the genome using the *STAR* aligner software (version 2.7) (Dobin et al. 2013) and intron
195 hints generated with the *bam2hints* tools within *AUGUSTUS*. *MAKER* v. 3.01.03 (Cantarel et
196 al. 2008), *SNAP* and *AUGUSTUS* (with intron-exon boundary hints provided from RNAseq)
197 were then used to predict for genes in the repeat-masked reference genome. To help guide
198 the prediction process, Swiss-Prot peptide sequences from the UniProt database were
199 downloaded and used in conjunction with the protein sequences from *D. grimshawi, D.*
200 *melanogaster, D. pseudoobscura, D. virilis, Z. africanus, Z. indianus, Z. tsacasi and Z.*
201 *tuberculatus* to generate peptide evidence in the *MAKER* pipeline. Only genes that were
202 predicted by both *SNAP* and *AUGUSTUS* were retained in the final gene sets. To help assess
203 the quality of the gene prediction, AED scores were generated for each of the predicted genes
204 as part of the *MAKER* pipeline. Genes were further characterized for their putative function by
205 performing a BLAST search of the peptide sequences against the UniProt database. tRNA
206 were predicted using the software *tRNAscan-SE* v. 2.05 (Chan and Lowe 2019).
207 Transcriptome completeness was assessed with *BUSCO* v. 4.0.5 (Manni et al. 2021) using the
208 eukaryota_odb10 list of 255 genes.
209
210 *Wild fly collections*
211
212 Flies were collected by aspiration and netting from Carter Mountain Orchard, VA (in 2017-2020
213 and from Hanover Peach Orchard, VA in 2019-2020. Flies were sampled from Coral Gables,

214 FL in June 2019 using traps baited with bananas, oranges, yeast, and red wine. See Table 1
215 for the number of individual flies sequenced from each location and timepoint. Flies were
216 frozen in 70% ethanol at -20°C (2017-2018) or dry at -80 °C (2019-2020) prior to sequencing.
217 Collections performed in July and August were called "early season." In 2019, the earliest
218 collections were not made until September (typically when *Z. indianus* abundance peaks,
219 Rakes et al. 2023), and were assigned "mid-season." Collections from October and November
220 were called "late season." For some analyses, the mid-season collection and early collections
221 were combined, as they were the first collections available each year.
222

Location	Latitude, longitude	Year	Season	Sampling date (# flies)	Number sequenced	Number after filtering
Coral Gables, FL, USA (FL)	25.535, -80.493	2019	-	1 Jun	25	24
Carter Mountain, Virginia, USA (VA-CM)	37.991, -78.472	2017	early	6 Jun (1) 22 Jun (7) 7 Jul (12)	20	17
		2017	late	9 Nov	20	19
		2018	early	5 Jul (2) 12 Jul (1) 19 Jul (1) 26 Jul (3) 2 Aug (1) 16 Aug (12)	20	20
		2018	late	1 Nov	20	19
		2019	mid	6 Sep	20	20
		2019	late	26 Oct	20	14
		2020	early	17 Jul	20	18
Hanover Peach Orchard, Virginia, USA (VA-HPO)	37.572, -77.266	2019	mid	3 Sep	20	19
		2020	early	16 Jul (5) 3 Aug (25)	30	29

223
224 **Table** 1. Sample information for new samples collected for this study. See Table S1 for
225 previously sequenced samples incorporated into this analysis.
226
227 *Individual whole genome sequencing*
228
229 The sex of each wild-caught fly was recorded, then DNA was extracted from individual flies
230 using the DNAdvance kit (Beckman Coulter, Indianapolis, IN) in 96 well plates, including an

231 additional RNase treatment step. DNA concentration was measuring using the QuantIT kit
232 (Invitrogen, Waltham, MA) and purified DNA was diluted to 1 ng/µL. Libraries were prepared
233 from 1 ng of genomic DNA using a reduced-volume dual-barcoding Nextera (Illumina, San
234 Diego, CA) protocol as previously described (Erickson et al. 2020). The libraries were
235 quantified using the QuantIT kit and equimolar ratios of each individual DNA were combined
236 for sequencing. The pooled library was size-selected for 500 bp fragments using a BluePippin
237 gel cassette (Sage Sciences, Beverly, MA). The pooled libraries were sequenced in one
238 Illumina NovaSeq 6000 lane using paired-end, 150 bp reads by Novogene (Sacramento, CA).
239
240 Existing raw reads from *Z. indianus* collections from North America, South America, and
241 Africa (Table S1; Comeault et al. 2020; Comeault et al. 2021) were downloaded from the SRA
242 from BioProject number PRJNA604690. These samples were combined with the new
243 sequence data and processed together with the same mapping and SNP-calling pipeline.
244 Overlapping paired-end reads were merged with *BBMerge* v. 38.92 (Bushnell et al. 2017).
245 Reads were mapped to the genome assembly described above using *bwa mem* v. 0.7.17 (Li
246 and Durbin 2009). Bam files for merged and unmerged reads were combined, sorted and de-
247 duplicated with *Picard* v. 2.26.2 (https://github.com/broadinstitute/picard).
248
249 We next used *Haplotype Caller* from *GATK* v. 4.2.0.0 (McKenna et al. 2010) to generate
250 a gVCF for each individual. We built a GenomicsDBI database for each scaffold, then used this
251 database to genotype each gVCF. We used *GATK's* hard filtering options to filter the raw
252 SNPs based on previously published parameters (*--filter-expression "QD < 2.0 || FS > 60.0 ||*
253 *SOR > 3.0 || MQ < 40.0 || MQRankSum < -12.5 || ReadPosRankSum < -8.0"*) (Comeault et al.
254 2020). We then removed SNPs within 20 bp of an indel from the output and removed all SNPs
255 in regions identified by *RepeatMasker*. We analyzed several measures of individual and SNP
256 quality using *VCFtools* v. 0.1.17 (Danecek et al. 2011). We removed 16 individuals with mean
257 coverage < 7X or over 10% missing genotypes. Next, we filtered SNPs with mean depths <10
258 or > 50 across all samples. We removed individual genotypes supported by 6 or fewer reads or
259 with more than 100 reads to produce a final VCF with 5,185,389 SNPs and 2,099,147 non-
260 singleton SNPs. See Table 1 and S1 for the final number of individuals included in the analysis
261 from each population. See Figure S2 for the average SNP depth per sampling time and
262 location.
263
264 *Sex chromosome and Muller element identification*
265
266 *samtools* v. 1.12 (Li et al. 2009) was used to measure coverage and depth of mapped reads
267 from individual sequencing. This analysis revealed that the five main scaffolds (all over 25 Mb
268 in length) had a mean depth of ~16X coverage in both males and females in our dataset,
269 except for scaffold 3, which had ~16X coverage in females but ~8X coverage in males,
270 suggesting it is the X chromosome (Figure S3). Some of the previously sequenced samples
271 had no sex recorded, so we used the ratio of X chromosome reads (scaffold 3) to autosome
272 (scaffolds 1, 2, 4 and 5) reads to assign sexes to those individuals. Individuals with a ratio
273 greater than 0.8 were assigned female, and ratios less than 0.8 were assigned male (Figure

274 S4). For two known-sex individuals, the sex recorded prior to sequencing did not match the
275 sex based on coverage; for those two samples we used the coverage-based sex assignment
276 for analyses. We used *D-GENIES* (Cabanettes and Klopp 2018) to create dot-plots comparing
277 the *Z. indianus* and *D. melanogaster* genome (BDGP6.46, downloaded from ensemble.org) to
278 confirm the sex chromosome identification and assign Muller elements to *Z. indianus*
279 autosomes (Figure S5, Table S2). Five additional scaffolds had lengths over 1 Mb. Scaffold 8
280 is the dot chromosome (Muller element F) based on sequence comparison to *D. melanogaster*
281 (Figure S5) and had similar coverage to the autosomes (Figure S3). Scaffolds 6,7,9, and 10
282 had reduced coverage (Figure S3) and contain mostly repetitive elements. Downstream SNP
283 calling and population genetic analysis included the five large scaffolds (named chromosomes
284 1-5 from largest to smallest) and excluded all smaller scaffolds.
285
286 *Testing for structural variants*
287
288 We used *smoove* v. 0.2.6 (Pedersen et al. 2020) to identify and genotype insertions, deletions,
289 and rearrangements in the paired-end sequencing data from all individuals as described in the
290 documentation. As an alternative approach to search for large structural variants, we used
291 linkage disequilibrium (LD) of randomly sampled SNPs from each chromosome to visually
292 inspect for linkage due to potential inversions. We generated a list of SNPs segregating in
293 each focal population with no missing genotypes and randomly sampled 4,000 SNPs from
294 each chromosome. We used the *snpgdsLDMat* function in *SNPRelate* to calculate LD between
295 all pairs of SNPs. LD heatmaps were created with the *ggLD* package
296 (https://github.com/mmkim1210/ggLD).
297
298 To define approximate inversion regions for SNP filtering, we looked for regions with
299 evidence of high long-distance linkage disequilibrium within North American samples. We note
300 that our purpose here was to roughly define inversion regions to exclude from population
301 structure analyses, not to precisely define inversion breakpoints, which will likely require further
302 long-read sequencing. For each SNP segregating in North America with complete genotyping
303 information, we randomly chose a second SNP that was 100, 200, 300, 400, or 500 kb away
304 from the focal SNP (+/- 5%). We calculated LD between the pair of SNPs. We then divided the
305 genome in 100 kb nonoverlapping windows and for each window determined if at least one
306 SNP in that window showed evidence of high long-distance LD ($R^2 > 0.75$) at any of the
307 sampled distances. Because some windows contain spurious examples of long-distance LD,
308 we defined inversion regions by looking for consecutive strings of at least 10 windows (1 Mb
309 total) containing high LD SNPs. This approach identified large potential inversion regions on
310 chromosomes 1, 2, 4, and 5 that corresponded to regions visually identified in LD heatmaps.
311 We masked SNPs in these regions (82.6 Mb total) for some downstream analyses.
312
313 *Population structure*
314
315 We conducted principal components analysis (PCA) using the R package *SNPRelate* v. 1.38.0
316 (Zheng et al. 2012) in R v. 4.1.1 (R Core Team) using a vcf that excluded singleton SNPs and

317 potential inversion regions. We LD pruned SNPs with minor allele counts of at least 3 (Linck
318 and Battey 2019) using *SNPgdsLDpruning* with an LD threshold of 0.2 and then calculated
319 principal components with *snpgdsPCA* using all four autosomes. For subsequent analyses, we
320 repeated the LD pruning within subsets of the data (North America only, or Carter Mountain,
321 VA only). We also calculated principal components using individual chromosomes; for the X
322 chromosome, only females were used in the analysis. The single fly collected in Kenya 2018
323 (Comeault et al. 2021) was an extreme outlier in the preliminary PCA and was excluded. We
324 conducted the initial analysis using all SNPs that met the filtering criteria and then conducted a
325 second analysis using SNPs that were masked for potential inversion regions as described
326 above. We conducted discriminant analysis of principal components using the *dapc* function in
327 package *adegenet* 2.1.10 (Jombart 2008; Jombart and Ahmed 2011). We used the
328 *optim.a.score* function to determine the number of PCs to include in the DAPC analysis.
329
330 We used *Plink* v. *1.9* (Purcell et al. 2007; Chang et al. 2015) to LD prune VCF files with
331 parameters (*--indep-pairwise 1000 50 0.2*) and used *ADMIXTURE* v. 1.3.0 (Alexander and
332 Lange 2011) to evaluate population structure. Using whole genome data not masked for
333 inversions, we calculated admixture for each chromosome separately. For the X chromosome,
334 only females were used. We tested up to *k*=10 genetic clusters and used cross-validation
335 analysis to choose the optimal *k* for each chromosome separately. We also ran ADMIXTURE
336 using all non-inversion autosomal SNPs together.
337
338 We calculated F_{ST} between Virginia samples and those from Florida or Africa using the
339 *snpgdsFST* function in *SNPRelate* for all SNPs with a minor allele count > 3. For the X
340 chromosome, only females were used in F_{ST} calculations. We used the same function to
341 calculate genome-wide, pairwise F_{ST} between all Virginia collections using autosomal SNPs
342 with putative inversions masked. To quantify relatedness between individuals, we used the
343 function *snpgdsibdKING* in *SNPRelate* v. 1.38.0 (Zheng et al. 2012) to determine the kinship
344 coefficients and probability of zero identity by descent for pairs of individuals using autosomal
345 SNPs with putative inversions masked. We used thresholds established in Thornton et al.
346 (2012) to classify relatedness between individuals. We used the *–het* function in *vcftools 0.1.17*
347 to calculate the inbreeding coefficient for each individual using non-inversion SNPs.
348
349 We generated phylogenetic trees using *Treemix* (Pickrell and Pritchard 2012). We
350 generated a vcf masked for inversions that contained only Carter Mountain and Florida
351 samples. We LD-pruned this vcf in PLINK 1.9 with *--indep-pairwise 100 10 0.2* and prepared
352 *Treemix* input files with custom scripts. We then ran 100 bootstrap replicates of *Treemix* with
353 zero migration edges, Florida as the outgroup, and arguments *–bootstrap -k 500.* We used
354 *PHYLIP* v. 3696 (Felsenstein 2005) to generate a consensus tree and support for each node.
355 We plotted a representative output in R using scripts from
356 https://github.com/andrewparkermorgan/popcorn/.
357
358 *Estimation of historic population sizes*
359

360 We used *smc*++ v. 1.15.4 (Terhorst et al. 2017) to estimate historic population sizes for several
361 subpopulations of individuals using chromosome 4 genotypes since this chromosome lacked
362 evidence of large structural rearrangements. We used individuals from each African location
363 and used the earliest sampling available for each year and Virginia orchard. We used *vcf2smc*
364 to prepare the input files for each autosome separately. We assigned each individual as the
365 "distinguished individual" and ran the analysis using all possible combinations of distinguished
366 individual as described in (Bemmels et al. 2021). We used cross validation to estimate final
367 model parameters with the option (*-cv –folds = number of individuals)*. We assumed a
368 generation time of 0.08 years (~12 generations per year) based on Nava *et al*. (2007), which
369 assumes year-round reproduction in tropical regions. We note that for Virginia populations
370 experiencing temperate conditions in recent years, 12 generations per year is likely an
371 overestimate due to the shortened breeding season.
372
373 *Selection scan*
374
375 We used *WhatsHap* v. 1.7 (Patterson et al. 2015) to perform read-based phasing of the full vcf
376 including singletons. To polarize the vcf for the genome wide selection scan relative to the
377 invasion, we reassigned the reference allele of the phased vcf as the allele that was most
378 common across all African individuals sequenced in previous studies. We calculated allele
379 frequencies using all African samples in *SNPRelate*, then used *vcf-info-annotator*
380 (https://vatools.readthedocs.io/en/latest/index.html) to assign the "ancestral" allele in the INFO
381 column. Lastly we used *bcftools* v. 1.13 (Danecek et al. 2021) to make simplified vcfs
382 containing only the GT and AA fields for each chromosome separately.
383
384 We used the R package *rehh* v. 3.2.2 (Gautier and Vitalis 2012) to conduct the selection
385 scan using integrated haplotype homozygosity score (IHS). The test measures the decay of
386 haplotype homozygosity to look for long, shared haplotypes that are signatures of selective
387 sweeps when a single haplotype rises to high frequency without being eliminated by
388 recombination (Sabeti et al. 2002; Voight et al. 2006). We used all flies from Virginia and
389 conducted the scan using phased, polarized vcfs for each individual chromosome. We used
390 the *haplo2hh*, *scan,* and *ihh2ihs* functions to implement the scan. For the X chromosome, we
391 only used a single haplotype for each male in the dataset to avoid double counting haploid
392 genotypes.
393
394 We also used *BayPass v. 2.41* (Gautier 2015) to calculate signals of selection
395 comparing flies from Virginia to those from Florida and Africa while accounting for population
396 structure via the XtX statistic. For this analysis, we used only females so that a single analysis
397 could be conducted across all chromosomes. We created separate vcf files for each population
398 and prepared *BayPass* input files using *vcftools –counts2*. We pruned these files for linkage
399 disequilibrium in *Plink* 1.9 using *--indep-pairwise 50 5 0.2.* We then ran *BayPass* according to
400 the user manual and modified code from (Whiting et al. 2021) to generate a core model and
401 covariance matrix and final XtX values. We used 10,000 simulated SNPs to define XtX outliers.
402

To look for shared signals across the F_{ST}, XtX and IHS selection/differentiation analyses, we used a window-based approach. We divided the genome into 1kb windows with a 500 bp step size and identified all windows that contained at least one SNP that fell in the top 99% of SNPs for the F_{ST}, XtX and IHS tests.

Genetic diversity statistics

Because we obtained variable sequencing coverage within and across populations (Figure S2) we used software designed for low coverage and missing data to analyze population genetic statistics in genomic windows. We used *pixy* v. 1.2.5 (Korunes and Samuk) to calculate Pi, F_{ST} and D_{XY} in 5 kb windows. Samples were grouped by collection location; only females were used for analysis of the X chromosome. We used *ANGSD* v. 0.941 (Korneliussen et al. 2014) to calculate Tajima's D. We first calculated genotype likelihoods from the bam files using arguments *-doSaf* and *-GL*. We then calculated Tajima's D and theta using the folded site frequency spectrum across 5 kb windows with 5 kb steps as described in *ANGSD* documentation using only female samples.

Data management and plotting

We used the R packages *foreach* (Microsoft and Weston 2017) and *data.table* (Dowle and Srinivasan 2019) for data management and manipulation and used *ggplot2* (Wickham 2016) for all plotting. The *ggpubfigs* (Steenwyk and Rokas 2021) and *viridis* (Garnier 2018) packages were used for color palettes.

Results and Discussion

Genome assembly and annotation

High quality genome assemblies and annotations are a critical component of tracking and controlling invasive species and understanding their potential for evolution in invaded ranges (Matheson and McGaughran 2022). We conducted Hi-C based scaffolding of a previously sequenced *Z. indianus* genome (Kim et al. 2021) to achieve a chromosome-level assembly. There were 1,014 scaffolds with an N50 of 26.6 Mb, an improvement from an N50 of 4.1-6.8 Mb in previous assemblies (Kim et al. 2021). The five main chromosomes (Figure S1, named in order of size from largest to smallest) varied in length from 25.7 to 32.3 Mb (total length of five main scaffolds = 146,062,119 bp), in agreement with *Z. indianus* karyotyping (Gupta and Kumar 1987; Campos et al. 2007). Chromosome 3 was identified as the X chromosome using sequencing coverage of known-sex individuals (Figure S3, S4). See Table S2 for assignment of *Z. indianus* chromosomes to Muller elements based on alignment to the *D. melanogaster* genome (Figure S5).

The annotation using RNAseq from larvae, pupae, and adults predicted 13,162 transcripts and 13,075 proteins, with 93% of 255 benchmarking universal single copy orthologs

446 (BUSCO) genes (Simão et al. 2015) identified as complete and an additional 1.2% of BUSCO
447 genes identified as fragmented. This transcriptome-based completeness estimate is lower than
448 the genome-based estimate of 99% complete (Kim et al. 2021) but is in line with other
449 arthropod genomes (Feron and Waterhouse 2022). Within the five main chromosomes, 24.6%
450 of sequences were repetitive; within the entire assembly including all smaller scaffolds, 41%
451 were repetitive. The five main chromosomes contain 11,327 predicted genes (87% of all
452 predicted), including 99.5% of all complete BUSCO genes. This improved genome resource
453 will be valuable for future evolutionary studies *of Z. indianus*, which is becoming an
454 increasingly problematic pest in some regions of the world (Allori Stazzonelli et al. 2023).
455
456 *Limited spatial or temporal population structure in North American Z. indianus*
457
458 To study spatial and temporal patterns of genetic variation in the seasonally repeated invasion
459 of *Z. indianus*, we resequenced ~220 individuals collected from two orchards in Virginia (Carter
460 Mountain Orchard and Hanover Peach Orchard) from 2017-2020, as well as one population
461 collected from Coral Gables, Florida in 2019. Because temperate locations such as Virginia
462 are thought to be recolonized by southern populations of *Z. indianus* each year (Pfeiffer et al.
463 2019; Rakes et al. 2023), we sampled both early in the season (~July-August) and late in the
464 season (~October-November) in each year to capture the founding event, population
465 expansion, and potential adaptation to the temperate environment.
466
467 We were first interested in studying geographic and temporal variation in population
468 structure in North American populations of *Z. indianus*. For this analysis, we incorporated
469 previous sequencing data from the Western Hemisphere and Africa (Table S1 and Comeault
470 et al. 2020). While previous studies have shown limited structure within North America
471 (Comeault et al. 2020; Comeault et al. 2021), we wanted to test for structure using deeper
472 sampling within introduced locations and with greater temporal resolution across the *Z.*
473 *indianus* growing season (Rakes et al. 2023). Our initial analyses of population structure using
474 principal components analysis (PCA) of the whole genome (Figures S6a) and individual
475 chromosomes (Figure S7a) and *ADMIXTURE* (Alexander and Lange 2011) analysis of
476 individual chromosomes (Figure S8) confirmed previous results that Western Hemisphere
477 samples are genetically distinct from African samples. To focus on potential structure within
478 invasive North American samples, we excluded the African samples and recalculated principal
479 components. North American samples fell into three large groups when considering PC1 and
480 PC2 (diagonal bands in Figure S6B), but these clusters generally did not correspond to
481 sampling locations. In single-chromosome PCA, North American samples formed clusters that
482 did not correspond to geographic locations for chromosomes 1, 2, 3, and 5; such patterns are
483 potentially indicative of inversions that influence genotypes of many SNPs simultaneously (Li
484 and Ralph 2019). This pattern was upheld in the *ADMIXTURE* analysis; notably, for
485 chromosomes 1, 2, and 5, many individuals showed ~50% ancestry assignment to different
486 clusters, which could reflect genotypes for large structural rearrangements. These findings led
487 to further investigations of potential structural polymorphisms (described below) and the

488 masking of SNPs potentially located in large chromosomal rearrangements to examine
489 population structure.
490
491 After removing regions of the genome that were potentially part of inversions (see
492 below), PC1 still separated Western Hemisphere and African samples (Figure 1a), and North
493 American samples remained tightly grouped for PCs 1-4, indicating most genetic variation is
494 found within African samples. Analysis of only North American samples revealed little genome-
495 wide separation of populations collected from different locations (Figure 1b), though some
496 Carter Mountain, Virginia individuals were outliers from the main cluster of points. Many
497 invasive species evolve complex population structures in the invaded range due to a
498 combination of bottlenecks, founder effects and rapid local adaptation (Koch et al. 2020;
499 Atsawawaranunt et al. 2023; García-Escudero et al. 2023). On the other hand, some invasive
500 species have more homogenous populations across widespread invaded ranges in eastern
501 North America (Friedline et al. 2019; Barrett et al. 2023). A high rate of migration between
502 orchards (occurring naturally or due to human-mediated transport) or large founding population
503 sizes could result in a lack of geographic differentiation between populations.
504
505

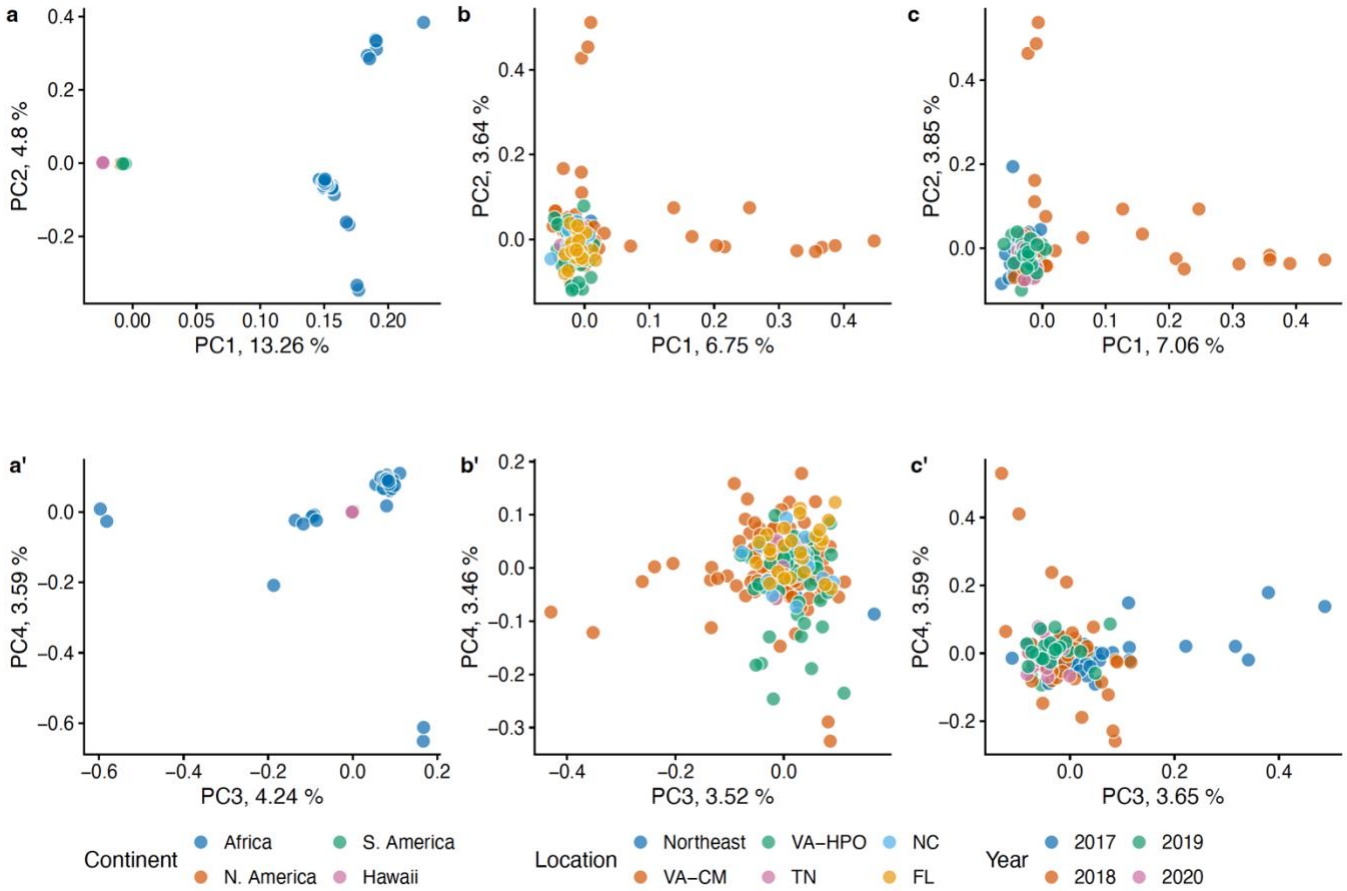

506
507 ***Figure 1: Principal component analysis of Z.* indianus *populations using***
508 ***autosomal SNPs outside of putative inversions reveals a lack of spatial or***
509 ***temporal population structure in invasive populations.*** *Top row shows PC1*

and PC2; bottom row shows PC3 and PC4. (a-a') All individuals (n=266), color coded by continent/locale of collection. South America, North America, and Hawaiian samples are all tightly clustered such that individual points are not visible. (b-b'). All North American individuals (n=224), color coded by collection site; HPO and CM are two orchards in Virginia; Northeast refers to samples from NY, NJ, and PA. (c-c') All individuals from Carter Mountain, Virginia (n=127), color coded by year of collection. For each analysis, only the individuals shown in the plot were included in the PC calculation.

We next hypothesized that founder effects during each recolonization event might lead to unique genetic compositions of temperate populations sampled in different years (Uller and Leimu 2011). We calculated principal components using only samples collected from Carter Mountain, VA in 2017-2020. Surprisingly, in these samples, we saw no evidence of population structure between years (Figure 1c), apart from some samples from 2018 that were divergent from the rest; we investigate potential causes of this pattern below. These data suggest that the founding fly populations in Virginia are relatively homogeneous each year at a genome-wide scale, but some years may contain genetically divergent individuals. This result is consistent with the lack of spatial population structure and likewise could indicate large founding populations or ongoing migration. Alternatively, the Virginia populations could be permanently established with little genetic differentiation year-to-year, though this possibility is not supported by field data from temperate locations (Rakes et al. 2023; Kohlmeier and Kohlmeier 2025).

ADMIXTURE revealed two ancestral clusters for global *Z. indianus* populations, separating Africa from North America (Figure 2). Adding increasing numbers of ancestral groups revealed genetic differentiation within North American samples, but this differentiation did not correspond to location or year of collection. Notably, with k=3, some individuals from Carter Mountain in 2018 separated from the other North American samples; these samples correspond to those that were outliers in the PCA. Collectively, our results are consistent with previous findings that African populations are distinct from those in the Western Hemisphere, and we find little evidence of genome-wide population structure over space or time within North American samples.

Figure 2: Admixture analysis of Z.* indianus *from different locations. *Each column is an individual, and colors represent assignment to distinct genetic clusters based on all autosomal SNPs outside of inversion. Each row represents a different number of ancestral genetic clusters (k = 2 to 6). FL=Coral Gables, Florida, VA-HPO = Hanover Peach Orchard, Virginia, VA-CM = Carter Mountain, Virginia. African sequences combine five geographic locations from Comeault et al. (2020 & 2021). Cross-validation analysis supported k=2 (top row) as the most likely number of ancestral groups.*

Structural polymorphism

The clustering of samples in the single-chromosome PCA (Figure S7), combined with many individuals showing ~50% assignment to genetic clusters within individual chromosomes (Figure S8), suggested that large structural variants may be segregating in *Z. indianus* (Li and Ralph 2019; Nowling et al. 2020). To look for evidence of structural variants via depressed recombination rates, we examined linkage disequilibrium (LD) from 4,000 randomly sampled SNPs on each chromosome. In North American samples, we discovered large blocks of LD spanning substantial portions of chromosomes 1, 2, 3, and 5 (Figure S9), potentially indicative of inversions (Fang et al. 2012; da Silva et al. 2019). However, there was no evidence of long-distance LD in these regions in the African samples (Figure S9). These results suggest inversions on chromosomes 1, 2, 3, and 5 are segregating in North America but are relatively rare in Africa. To approximately define the boundaries of these inversions, we calculated LD

565 for random pairs of SNPs that were 100-500 kb apart on each chromosome. This analysis
566 similarly identified large regions containing elevated long-distance LD on chromosomes 1, 2, 4,
567 and 5 (Figure S10A). We compared the results of the LD analysis to potential inversions called
568 using paired-end data by *smoove* but found little correspondence (Figure S10B, compare gray
569 boxes to yellow boxes). As such, we use the LD-based data to mask potential inversion
570 regions for population structure analyses described above.
571
572 Given the relative chromosome sizes in the genome assembly, the linkage blocks on
573 chromosomes 2 and 5 likely correspond to the previously described inversions *In(V)B* and
574 *In(II)*A, respectively (Ananina et al. 2007). Since chromosome 1 is the longest chromosome in
575 our assembly, the linkage likely correspond to the complex *In(IV)EF* polymorphism, made up of
576 two overlapping inversions (Ananina et al. 2007); different genotypic combinations of two
577 inversions could explain the six distinct clusters seen in the chromosome 1 PCA (Figure S7b).
578 The X chromosome has three described inversions in *Z. indianus* (Ananina et al. 2007), which
579 may explain to the complex pattern of linkage observed in North American samples on this
580 chromosome (Figure S9, S10) and the clustering of North American samples in the
581 chromosome 3 PCA (Figure S6B,C). Major chromosomal polymorphisms are known to be
582 important for local adaptation and phenotypic divergence in a wide variety of species (Joron et
583 al. 2011; Küpper et al. 2016; Lee et al. 2016; Huang et al. 2020; Nunez et al. 2024), including
584 inversions that facilitate invasive phenotypes (Galludo et al. 2018; Tepolt and Palumbi 2020;
585 Tepolt et al. 2022; Ma et al. 2024). These inversions may be new to North America, or they
586 may have been present at low frequency in the bottlenecked population that founded *Z.*
587 *indianus* populations in the Western Hemisphere but then experienced subsequent selection in
588 the invaded range. Alternatively, they have arisen in a currently unsequenced population and
589 then been introduced to the Western Hemisphere. Further characterization of these inversions
590 via additional sequencing and phenotypic characterization to determine whether they influence
591 *Z. indianus*' survival or fitness in the invaded range will be a rich area for future studies.
592
593 *Recolonization, bottlenecks and seasonal dynamics in* Z. indianus
594
595 Invasive species typically experience a genetic bottleneck due to small founding
596 population sizes (Barrett 2015; Estoup et al. 2016). We hypothesized that North American
597 populations would show reduced effective population size (N_e) relative to African populations,
598 and that Virginia populations would show a further, more recent reduction in N_e relative to
599 Florida populations as the result of a secondary population bottleneck upon temperate
600 recolonization. We estimated historic population sizes using *smc++* (Terhorst et al. 2017) using
601 data only from chromosome 4, which lacks large inversions (Figure 3a). Our prediction was
602 correct with respect to Africa vs North America: African populations show historical fluctuations
603 but population sizes typically in the range of ~ 10^4-10^7 individuals (10^6-10^7 for the past ~1,000
604 years). However, introduced populations in North America demonstrated a dramatic reduction
605 in population size in the past ~100 years, perhaps reflecting a bottleneck following colonization
606 of Brazil in the late 1990s (Yassin et al. 2008) and consistent with the previously described
607 loss of genetic diversity in invasive populations (Comeault et al. 2020). This contraction is

608 followed by a rebound as introduced populations expanded over the past several decades.
609 Overall, the ancestral population sizes for Virginia and Florida were quite similar with
610 overlapping ranges of the estimates, and our prediction of reduced recent population sizes in
611 Virginia relative to Florida was not well-supported. Given our limited sample sizes and potential
612 differences in the number of generations per year in temperate and subtropical environments,
613 detecting fine-scale differences in very recent population fluctuations may be beyond the
614 detection ability of the software; *smc++* becomes less accurate at timescales less than ~333
615 generations (~26 years for year-round populations of *Z. indianus*) (Patton et al. 2019). Virginia
616 populations could be colonized by a large number of individuals, or they may represent
617 admixed populations reflecting individuals from multiple sources, producing larger effective
618 population sizes than would otherwise be expected if recolonization occurs from a single
619 source population undergoing a bottleneck. Admixture and gene flow are important factors
620 fueling genetic diversity and invasiveness in introduced species (McGaughran et al. 2024) and
621 could potentially contribute to *Z. indianus'* local success following each recolonization event.
622

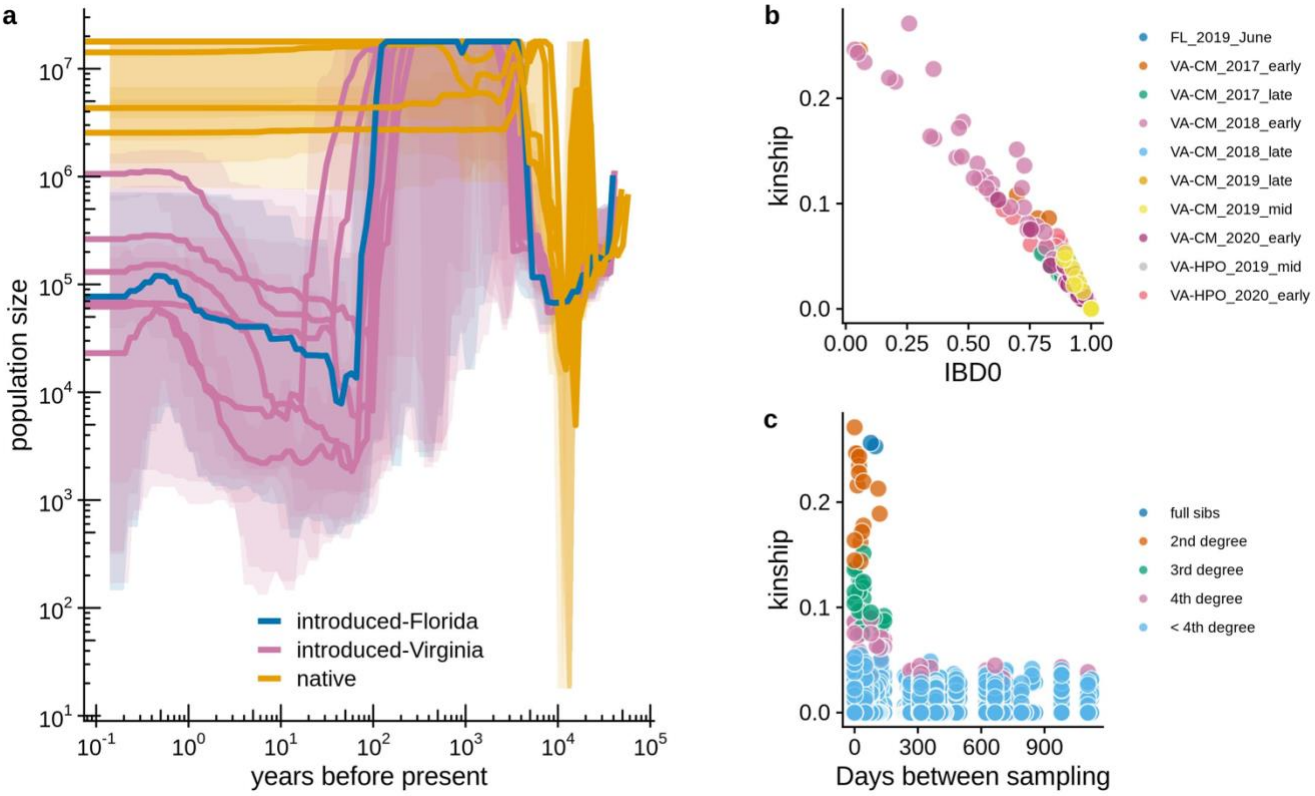

623
624
625 ***Figure 3: Demographic effects of bottlenecks in* Z. indianus *populations*** *a)*
626 *Population history reconstruction with* smc++ *using genotypes from chromosome*
627 *4, which lacks inversions. Introduced-Virginia flies were collected in the early-mid*
628 *season (June-September) from two Virginia orchards in 2017-2020 (n=6*
629 *populations grouped by orchard and year). Native populations are five distinct*
630 *African populations (Kenya, Zambia, Senegal-Forest, Senegal-Desert, and Sao*
631 *Tome [Comeault et al. 2020]). Shaded ribbons show minimum and maximum*
632 *population sizes estimated in cross-validation analysis. b) Kinship and probability*

633 *of zero identity by descent for pairs of individual flies from the same collection*
634 *location and season within North America calculated with non-inversion*
635 *autosomal SNPs. c) Kinship coefficients for pairs of individual flies collected at*
636 *Carter Mountain Orchard, Virginia, as a function of the number of days between*
637 *sampling. Relatedness was assigned according to thresholds from Thornton et*
638 *al. (2012).*
639
640 We additionally tested for bottlenecks by looking for the presence of relatives within our
641 samples, which might be a product of small founding populations. Using two measures of
642 genetic similarity, we discovered many pairs of related flies in our dataset (Figure 3B). Most
643 dramatically, many flies collected in 2018 appeared to be close relatives (Figure S11),
644 consistent with the separation of some 2018 samples in the PC and *ADMIXTURE* analyses
645 (Figures 1c and 2). In collections from late July and early August 2018, 26 pairs of close
646 relatives involving 13 individual flies were collected. Of those, 21 pairs of relatives were
647 collected on different days, suggesting the relatedness was not solely a sampling artifact due
648 to collecting relatives in the same microhabitat of the orchard. The effect of this apparent
649 bottleneck was sometimes retained throughout the growing season, as a pair of full sibs was
650 sampled 77 days apart in 2018, two pairs of second-degree relatives were sampled over 110
651 days apart in 2018, and two pairs of third-degree relatives were sampled 140 days apart in
652 2017 (Figure 3c). Given that *Z. indianus* are collected in small numbers early in the season
653 (Rakes et al. 2023) and 2017 and 2018 had particularly early captures (Table 1), we thought a
654 small founding population size followed by inbreeding could produce individuals sampled
655 distantly in time that still show close genetic similarity. However, we did not find any significant
656 difference in inbreeding coefficients between flies sampled at different time points at Carter
657 Mountain (ANOVA, $F(6,120) = 1.79$, $P = 0.106$). Instead, flies may live for a relatively long time
658 or have slower generations in the wild, allowing us to capture close relatives separated by
659 longer time periods. However, we note that the same pattern was not seen in every year of our
660 collections, suggesting that colonization dynamics might differ dramatically from year to year,
661 which is expected if recolonization occurs due to chance events each year.
662
663 A founder effect could generate temporal population structure by creating populations
664 that were more similar within a year than between years, creating a positive relationship
665 between F_{ST} and the elapsed time between collections (Bergland et al. 2014). We tested this
666 prediction with samples collected from Carter Mountain, Virginia over four years and found a
667 weak, positive correlation between F_{ST} and the time between sample collections for
668 comparisons that excluded the unusual 2018 collection containing many relatives (linear
669 model, df=19, $R^2 = 0.423$, P=0.009, Figure S12). This finding is consistent with trends
670 observed in *D. melanogaster,* which experiences a strong overwintering bottleneck and shows
671 temporal patterns of differentiation (Bergland et al. 2014; Nunez et al. 2024). Since this finding
672 could be caused by an overwintering bottleneck or a recolonization bottleneck, we further
673 investigated population relationships over time.
674

We used discriminant analysis of principal components (DAPC) and phylogenetic trees to look at relationships between flies captured at Carter Mountain, Virginia, over time relative to the population from Florida. In North America, *Z. indianus* was first found in Florida and was later found northwards (Linde et al. 2006; Pfeiffer et al. 2019). If flies are permanently established in Virginia, we predict that the Virginia populations would become progressively more different from Florida over time in a “stepping-stone” like pattern as each population evolves independently. If flies recolonize each year with small founding population sizes, we expect populations to be more similar to Florida in some years than others due to chance. The predictions of recolonization were supported by the DAPC analysis, which showed that the 2019 sample shared the most overlap with Florida, while 2018 was the most different (Figure 4a), and there was no clear pattern of temporal differentiation. We also used *Treemix* (Pickrell and Pritchard 2012) and *PHYLIP* (Felsenstein 2005) to build a consensus phylogenetic tree from 100 independent bootstraps of the same dataset. The topology of the consensus tree (Figure 4b) was not consistent with stepwise divergence of the populations over time; the two earlier timepoints formed a clade and the two later timepoints formed a clade, though the node for the 2019-2020 divergence was not well supported. The drift parameter was greater in 2017 and 2018 than it was 2019 and 2020, suggesting that populations collected later in time were more similar to Florida than those collected earlier in time. This result is consistent with a recolonization model in which the founding population is randomly more representative of the source population in some years than others, with smaller and earlier founding events in 2017 and 2018 potentially leading to greater genetic drift. Additional demographic simulations will likely be required to more definitively determine the colonization dynamics of *Z. indianus*.

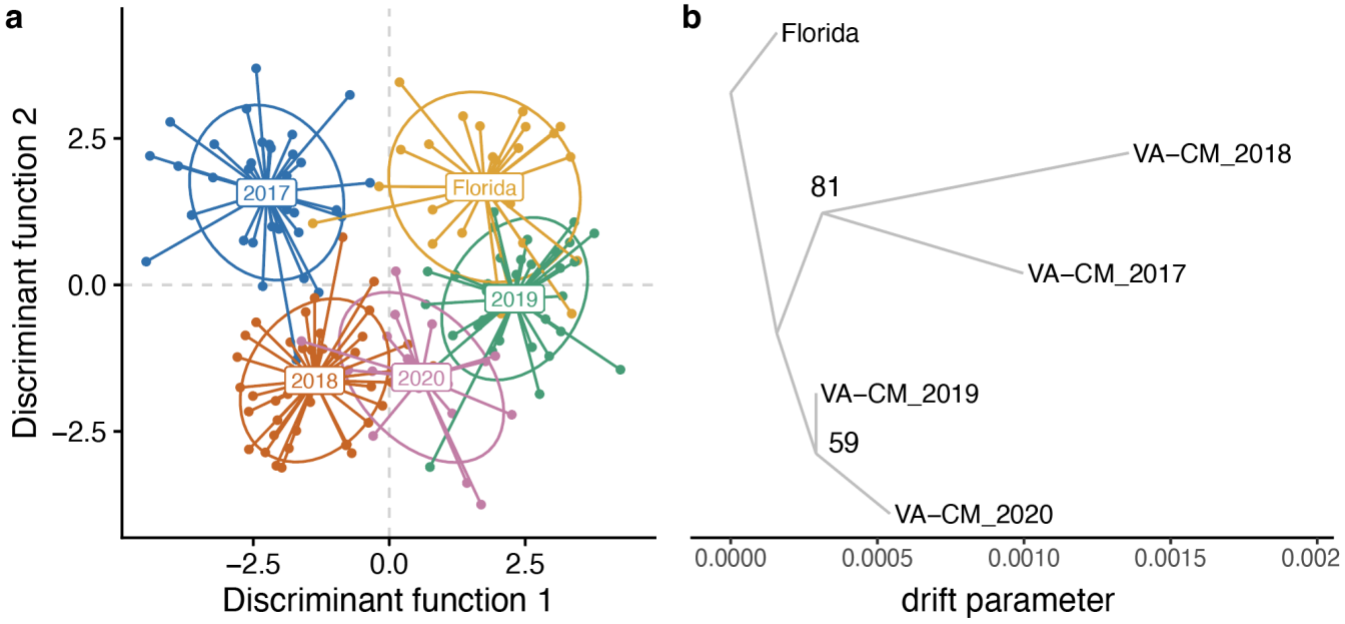

Figure 4: DAPC and* Treemix *analyses suggest* Z. indianus *recolonizes Virginia each year. *All analyses were conducted with autosomal SNPs outside of inversions. a) Discriminant analysis of principal components (DAPC) of samples from Florida and four years of sampling from Carter Mountain, Virginia.*

703 *b) Results of a single* Treemix *run representative of the consensus tree topology*
704 *from PHYLIP; bootstrap support values from 100 trees are given at nodes.*
705
706 *Signals of recent selection in Z. indianus near potential pesticide resistance genes*
707
708 We tested for signals of recent natural selection in temperate *Z. indianus* populations from
709 Virginia. We compared Virginia populations to those from Africa to test for broader invasive-
710 native population differentiation and compared Virginia to Florida to look for potentially more
711 recent temperate adaptation. We measured three statistics: SNP-level F_{ST} comparing all flies
712 collected Virginia to those from Florida or Africa; the XtX statistic from *BayPass* (Gautier 2015)
713 to test for selection in the presence of population structure, and integrated haplotype
714 homozygosity score (IHS) to look for long, shared haplotypes that are signatures of recent
715 selective sweeps when a single favorable haplotype rises to high frequency (Sabeti et al.
716 2007). We note that our approach would not detect sweeps involving multiple alleles from
717 standing variation (soft sweeps; Messer and Petrov 2013; Garud et al. 2015), which could be
718 an important potential component of *Z. indianus* evolution given the high levels of genetic
719 diversity found in invasive populations (Avalos et al. 2017; Comeault et al. 2020). To compare
720 results across tests, we looked for 1 kb windows containing SNPs that fell in the top 1% of all
721 three tests. As expected given the high degree of population structure, SNPs with high F_{ST}
722 between Africa and Virginia were widespread across all chromosomes, and F_{ST} was
723 particularly high on the X chromosome (Figure 5a). This observation is in line with the findings
724 of Comeault et al. (2021), who showed that many X-linked scaffolds showed signs of selection
725 in invasive populations, and we suggest this pattern is likely related to the smaller effective
726 population size for X chromosomes (Ellegren 2009) and the presence of several inversions on
727 this chromosome (this study; Ananina et al. 2007). After accounting for population structure
728 with *BayPass*, the signal remained high throughout most of the X chromosome, but several
729 peaks of potential selection were resolved on the autosomes, including prominent peaks on
730 chromosomes 2 and 5 (Figure 5c). These peaks corresponded to windows with long, shared
731 haplotypes in Virginia populations (high IHS scores, Figure 5e). The complex population
732 structure and broadly elevated signals of divergence and selection on the X chromosome
733 made it difficult to investigate candidate loci further. In contrast, only a small number of
734 autosomal windows were found to contain elevated signals for all three tests, so we focused
735 on the two autosomal windows that had the most pronounced signals for the *BayPass* and IHS
736 analysis: Chromosome 2 at ~26.6 Mb and Chromosome 5 at ~7.9 Mb (asterisks in Figure 5e).
737

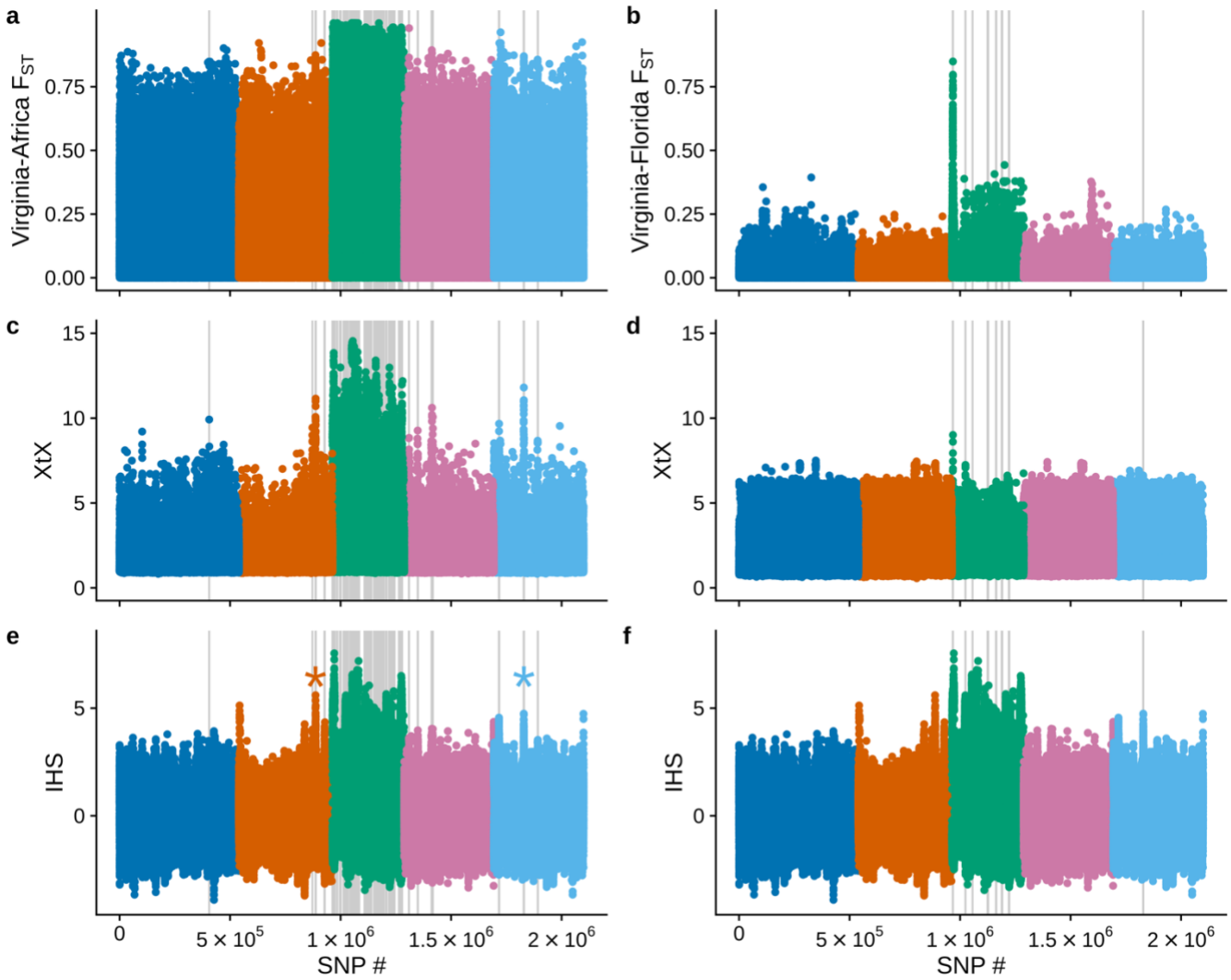

Figure 5: Signals of differentiation and selection in temperate* Z. indianus *populations. *a-b) Genome-wide F_{ST} comparing individual flies sampled in Virginia (n= 175) to all flies sampled in Africa (a, n = 34) or Florida (b, n = 26); colors indicate chromosomes 1-5 in order. Only females were used for the X chromosome analysis (chromosome 3, green). c-d)* BayPass *XtX statistic for comparisons of females from Virginia and Africa (c) and Virginia and Florida (d). e-f) Integrated haplotype homozygosity score (IHS) testing for long, shared haplotypes in all flies collected in Virginia. The IHS datapoints in panels (e) and (f) are the same but presented twice to show alignments with each analysis above. Gray vertical lines indicate locations of 1 kb windows that contain F_{ST}, XtX, and IHS scores in the top 1% genome-wide; windows were calculated separately for the Virginia-Africa and Virginia-Florida comparisons. Asterisks in panel (e) indicate the shared peaks on chromosomes 2 (orange) and 5 (light blue) discussed in the text and examined in Figure 6.*

755 We examined the genes annotated in each of these outlier regions and found
756 that both regions included genes in the cytochrome P450 pathway, which is involved in
757 detoxifying endogenous and exogenous compounds including synthetic pesticides
758 (Scott et al. 1998). The IHS peak on chromosome 2 is found near the *Z. indianus*
759 homolog of *D. melanogaster cpr*, a cytochrome P450 reductase essential for electron
760 transfer in the detoxification activities of cytochrome P450 genes (Hannemann et al.
761 2007). Decreased *cpr* expression has been linked to susceptibility to pesticides in a
762 variety of insect pests and disease vectors (Lycett et al. 2006; Wang et al. 2016; He et
763 al. 2020; Shi et al. 2021; Wang et al. 2025). A proline-to-leucine polymorphism in *cpr*
764 has an XtX score of 7.63, is not found in Africa, and has a frequency of 0.57 in Virginia.
765 Two other SNPs upstream of *cpr* also have large allele frequency differences between
766 Virginia and Africa, offering interesting candidates for further study that might influence
767 gene regulation.
768
769 The IHS peak on chromosome 5 is near a cluster of five cytochrome P450
770 genes. Although additional work will be required to resolve CYP gene orthologs and
771 paralogs in *Z. indianus*, the cluster contains several *Cyp6* genes. One of the largest
772 signals of selective sweeps in the *D. melanogaster* genome is found in *Cyp6g1* (Garud
773 et al. 2015); alleles are *Cypg1* are associated with resistance to DDT and
774 neonicotinoids (Daborn et al. 2001; Schmidt et al. 2010). Therefore, mutations in *Z.*
775 *indianus CYP6* genes might also be involved in insecticide resistance. For example, in
776 this region, missense variants in *Cyp6a9* and *Cyp317a1* have large allele frequency
777 differences between Virginia and Africa; *Cyp317a1* was associated with permethrin
778 resistance in the Drosophila Genetic Reference Panel (Battlay et al. 2018). *Z. indianus*
779 is a substantial crop pest in Brazil, and several studies have indicated Brazilian *Z.*
780 *indianus* populations may have evolved some degree of pesticide resistance in
781 response to the use of organophosphorous compounds to protect fig crops (Galego and
782 Carareto 2010; de Oliveira Rios et al. 2024). Although *Z. indianus* is not currently
783 categorized as a pest in the United States (Animal and Plant Health Inspection Service,
784 2025) and is not an active target of management in eastern US orchards, many
785 orchards use insecticides to control *D. suzukii* (Tait et al. 2021) and other arthropod
786 pests. Controls for *D. suzukii* are often applied at the time of fruit ripening, which means
787 that other species such as *Z. indianus* that are present during and after ripening may
788 also be impacted by chemical control. Chemicals applied closer to the time of ripening
789 may be more likely to remain on the overripe and decomposing fruit typically used as a
790 breeding substrate for *Z. indianus.* Further investigation will be required to determine if
791 mutations at these loci cause differences in pesticide resistance between African and
792 North American flies. Insecticide resistance is a major challenge in the control of
793 invasive insect pests (Siddiqui et al. 2023), and characterizing resistance may be
794 important for future control of *Z. indianus*.
795
796 We confirmed the potential signal of selective sweeps by looking at haplotype
797 structure in these two regions. Each region of high XtX score (Figure 6a-b) was

characterized by a broad peak of extended haplotype homozygosity (EHH) specific to the allele found in invasive populations (Figure 6c-d), demonstrating that the candidate alleles have a slow decay of haplotype homozygosity. Visualization of the alleles found in each haplotype showed long haplotype blocks in North American populations that were not found in Africa (Figure 6e-f); SNPs within these blocks demonstrate high linkage disequilibrium in North American flies (Figure 6g-h). Additional analysis revealed these haplotypes were found in Colombia, suggesting they may have originated after *Z. indianus* arrived in the Western Hemisphere but may predate *Z. indianus's* arrival in North America. In invasive copepods, haplotypes under selection in the invasive range are ancestral polymorphisms under balancing selection in the native range (Stern and Lee 2020). A similar situation was found for a balanced inversion polymorphism that fuels invasion in invasive crabs (Tepolt and Palumbi 2020; Tepolt et al. 2022). However, ancestral polymorphisms selected in the invaded range does not appear to be the case in *Z. indianus*, as the haplotypes from North America were not found in African flies. These novel haplotypes could be new mutations or derived due to hybridization/introgression from another species or divergent population; hybridization can be an important evolutionary force in invasive species (Ellstrand and Schierenbeck 2000; Fournier and Aron 2021). The *Zaprionus* genus shows signals of historic introgression among several species, though *Z. indianus* was not directly implicated in a previous analysis (Suvorov et al. 2022). Therefore, two major haplotypes not found in Africa have been selected in Florida and Virginia populations, though the source of these haplotypes remains to be determined.

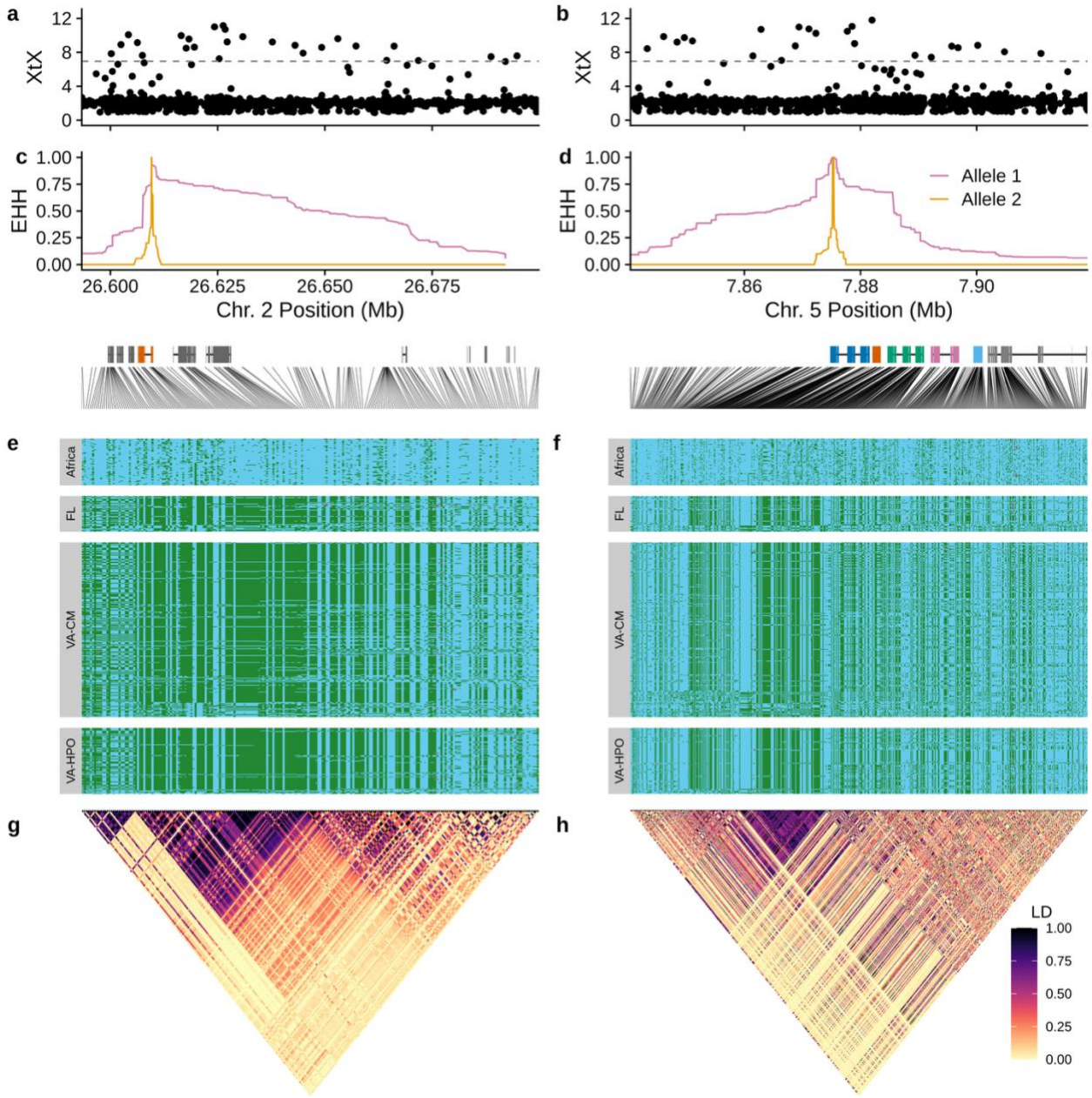

Figure 6: Haplotypes near potential pesticide resistance genes with signals of selection and differentiation*. a-b) BayPass XtX statistics for individual SNPs comparing Africa and Virginia populations (see Figure 5a) for peaks on chromosomes 2 (a) and 5 (b). Horizontal lines indicate the 99.9% quantile of XtX scores from 10,000 simulated SNPs. c-d) Extended haplotype homozygosity for the SNP with highest IHS score at each locus (Chr. 2: 26,609,601 and Chr. 5: 7,875,359). The locations of annotated genes are shown below the x-axis. In panel (c) the gene highlighted in orange is* Cytochrome P450 reductase *(*cpr*). In (d) the genes highlighted in color are a cluster of five* Cytochrome P450 *genes (predicted as* Cyp6a14, Cyp6a22, Cpy317a1, Cyp6a13, Cyp6a9 *from left to right). Gray lines connect SNP order for panels below to physical locations on chromosomes. e-f) Haplotypes at each locus: each horizontal row shows*

835 *genotypes for a single haploid chromosome phased with read-backed phasing.*
836 *Blue indicates the allele more common in African populations and green is the*
837 *other allele. Missing genotypes are shown in gray. Panel e shows 223 SNPs and*
838 *panel f shows 599 SNPs. g-h) LD (R^2) heatmaps for all SNPs for each haplotype*
839 *demonstrate linkage in North American flies.*
840
841 To explore population genetic signals around these potential regions of selection, we
842 broadly grouped flies into three populations—Africa, Florida, and Virginia—and calculated
843 population genetic statistics in 5 kb non-overlapping windows. F_{ST} between African and North
844 American populations fell in the top 99% of all autosomal windows for both regions (Figure 7a-
845 b), suggesting a high degree of genetic divergence. However, absolute genetic divergence
846 (D_{xy}) between African and North American populations was not especially elevated in these
847 windows (Figure 7c-d). Nucleotide diversity (pi) was in the lowest 1% of all autosomal windows
848 for North American samples (Figure 7e-f), as predicted for a sweep that results in shared
849 haplotypes across many individuals. Tajima's D was also negative and in the lowest 1% of all
850 autosomal windows for North America, indicative of a recent sweep (Figure 7g-h). Tajima's D
851 was negative in Africa for these regions, but was it negative across the entire genome (Figure
852 S15), likely due to combining genetically disparate subpopulations into a single population for
853 this analysis, producing an excess of rare variants. Relative sequencing depth showed
854 fluctuations in North American samples that were not seen in Africa (Figure 7h-i), suggesting
855 the possibility of copy number variants may exist in both regions. Collectively, these tests
856 provide additional evidence that both regions may have been subject to recent selective
857 sweeps.
858

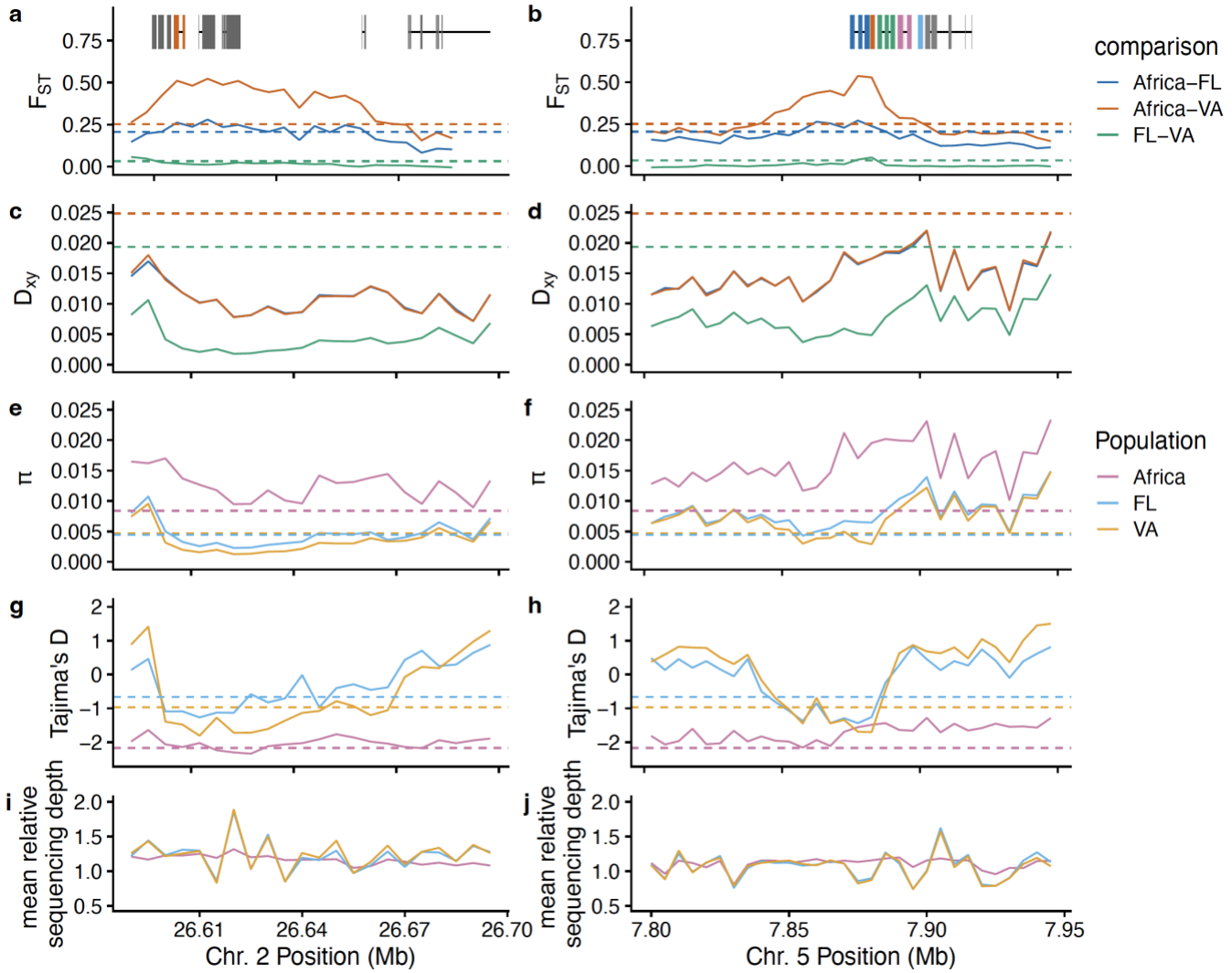

Figure 7: Population genetic statistics for the regions surrounding haplotypes on chromosomes 2 and 5. *All statistics were calculated for 5 kb, non-overlapping windows. Panels on left focus on the chromosome 2 region containing* cpr*, and the panels on right focus on the chromosome 5 region containing several* Cyp *genes. Gene locations are shown at the top using same color scheme as in Figure 6. a-b)* F_{ST} *comparing combinations of flies from Africa, Virginia (both focal orchards combined) and Florida. c-d) Absolute nucleotide divergence (*D_{xy}*) for the same comparisons. For a-d, horizontal lines indicate 99*th *percentile of all autosomal windows. e-f) Nucleotide diversity (π) for each population. g-h) Tajima's D for the three populations. For e-h, horizontal lines indicate bottom 1*st *percentile of all autosomal windows. i-j) Average sequencing depth per window relative to the mean depth for the entire chromosome. Relative depths were averaged for all individuals in each population. See Figure S13 for whole-genome visualization of the same statistics.*

877 For comparison, we also examined genetic diversity and population divergence across
878 the genome (Figure S13) and observed that the X chromosome is an outlier in many regards.
879 Divergence between Africa and North American samples is greater on the X chromosome
880 (Figure S13A-B). As previously described (Comeault et al. 2020; Comeault et al. 2021), the X
881 chromosome has reduced genetic diversity relative to autosomes, especially in invaded
882 populations (Figure S13C). X chromosomes have smaller effective population sizes in species
883 with XY sex determination systems and often experience more extreme loss of genetic
884 diversity upon population contraction (Ellegren 2009). Tajima's D is mostly positive in North
885 American autosomes, indicative of a strong bottleneck in North American flies. However,
886 Tajima's D fluctuates between strongly positive and strongly negative in North American
887 populations along the X chromosome (Figure S13D). These findings, combined with many
888 regions with high haplotype homozygosity on the X chromosome (Figure 5e-f), suggest
889 complex evolutionary dynamics on the X that warrant further investigation. Further global
890 sampling and sequencing of X chromosomes with long reads to resolve inversion genotypes
891 and CNVs may offer insight towards the potential role of X-linked variants in fueling the
892 ongoing invasion of *Z. indianus*.
893
894 We lastly compared Virginia to Florida to test for possible recent adaptation within the
895 invasive range of *Z. indianus*. Virginia has a temperate, seasonal climate with a relatively
896 limited variety of cultivated produce, and southern Florida is subtropical with an abundance
897 and diversity of fruits throughout the year. Other factors such as diseases, insecticide use, and
898 competing species may also differ widely between locales. In the absence of genome-wide
899 population structure, genomic regions differentiated between these locations are candidates
900 for local adaptation. We observed elevated F_{ST} throughout much of the X chromosome, with a
901 pronounced peak at 690 kb (Figure 5b); this peak was found near the most pronounced peaks
902 in the XtX (Figure 5d) and IHS (Figure 5f) statistics. Examination of this region of the genome
903 showed several long, shared haplotypes with high linkage in North American populations
904 (Figure S14); in particular, one haplotype is nearly fixed in Virginia but is segregating in
905 Florida. It is possible that this haplotype is associated with one of the structural variants on the
906 X, and differences in inversion allele frequencies between Florida and Virginia could be driving
907 these patterns. We examined population genetic signals in the region of highest F_{ST} (Figure
908 S15) and determined that despite high F_{ST} from ~550-650 kb (Figure S15A), D_{xy} between
909 Florida and Virginia was not high in this region, nor were nucleotide diversity (Figure S15C) or
910 Tajima's D (Figure S15D) particularly low. In fact, immediately adjacent to the region of high
911 FST was a region of nearly zero divergence between Florida and Virginia from ~700-800 kb
912 (Figure S15A-B). This region of low divergence had low nucleotide diversity (Figure S15C) and
913 negative Tajima's D (Figure S15D), indicating it could be a sweep in North America. However,
914 it was immediately adjacent to a region of irregular sequencing depth (Figure S15E),
915 suggesting the signals we observed could be confounded by read mapping artifacts.
916
917 Because the region of high F_{ST} is located near the end of the X chromosome and may
918 be telomeric and/or centromeric, we more closely examined the normalized depth of
919 sequencing coverage and presence of repetitive elements (Figure S16). This region contained

920 a large repetitive element (Figure S16A), and sequencing depth was variable across
921 populations (Figure S16B), suggesting structural variants such as duplications or deletions
922 could be influencing mapping and population genetic statistics in this region. For example, at
923 ~610 kb, Florida samples had greater depth than Virginia, but from ~625kb-650kb, Virginia
924 samples had greater depth than Florida or Africa. All samples had low coverage near the
925 repetitive element. These findings suggest copy number variation near repetitive elements at
926 these loci might contribute to the Florida-Virginia divergence; whether the divergence is an
927 artifact due to sequence misalignments or due to real copy number variation will require further
928 analysis with long-read sequencing. The region of highest divergence between Florida and
929 Viriginia contains ~6 genes, including the gene *yin/opt1*, which is important for absorption of
930 dietary peptides in *D. melanogaster* (Roman et al. 1998). If the Florida-Virginia divergence in
931 this region is not a sequencing artifact, allelic differences within the invasive range in this gene
932 could be involved in adaptation to new diets in new environments.
933
934 **Conclusions**
935
936 In addition to posing economic, health, and environmental threats, invasive species also
937 serve as outstanding models for studying rapid evolution in new environments. Here we report
938 an improved genome assembly and annotation for *Z. indianus*, an introduced drosophilid that
939 is thought to repeatedly recolonize temperate environments each year and is a potential crop
940 pest. We use it for a preliminary assessment of potential rapid evolution and genetic variation
941 in the early stages of invasion. We show that recolonization is likely a stochastic process
942 resulting in different evolutionary dynamics in different years, even within a single orchard. This
943 finding demonstrates broad sampling is important for invasive species that are repeatedly
944 introduced or have multiple introduced populations that may undergo different evolutionary
945 trajectories in different years or different locations. While some founding populations may be
946 small, several population genetic patterns we observe could be explained by ongoing gene
947 flow with the source population or between temperate populations following recolonization,
948 suggesting gene flow that spreads and maintains favorable alleles could be an important
949 component in *Z. indianus*'s widespread success, as it is for many invasive species (Díez-del-
950 Molino et al. 2013; Medley et al. 2015; Arredondo et al. 2018). Demographic simulations and
951 additional whole genome data will be required to better describe the recent histories of and
952 potential gene flow between invasive populations and to infer colonization routes within North
953 America.
954
955 Though we find limited population structure across space or time in introduced North
956 American populations, we identified two selective sweeps in regions containing genes in the
957 cytochrome P450 pathway, implicating pesticide resistance as a potential cause of recent
958 sweeps in the invaded range. These haplotypes were not found in African samples, suggesting
959 these alleles may have evolved in the past ~25 years since *Z. indianus* invaded the Western
960 Hemisphere, though we can't rule out their origin in another undescribed population. Additional
961 work will be required to characterize insecticide resistance in *Z. indianus* and compare
962 resistance across alleles to test the hypothesis that these alleles are involved in a recent

963 sweep involving pesticide resistance. We also find a region on the X chromosome that shows
964 potential evidence of a selective sweep in temperate regions, potentially due to copy number
965 variation, but the signal could be an artifact of genome assembly issues and sequencing near
966 repetitive elements. Further investigation will be required to resolve the signals in this region.
967 Studying how genetic variation in this region of the genome influences survival in temperate
968 environments will be an important direction of future research. We additionally find that the X
969 chromosome has an unusually complex evolutionary history in *Z. indianus*. It may have several
970 segregating inversions and CNVs, has strong signatures of selection, and shows regions of
971 high divergence both between African and North American populations and within North
972 America. Specifically, long-read sequencing strategies will be important to understand likely
973 inversions both on the X and throughout the *Z. indianus* genome that are common in the
974 invaded range. Large inversions can link together adaptive alleles and are often important
975 drivers of evolution in rapidly changing environments (Thompson and Jiggins 2014), so these
976 regions will be important to track over larger spatial and temporal scales in future studies.
977
978 These results underscore the complexity of genetic dynamics during invasions and the
979 need for further studies to explore the adaptive potential and ecological impacts of *Z. indianus*
980 in its invasive range. *Z. indianus* provides a unique system in which we can study independent
981 invasion events across multiple years and locations. One limitation of our study is sample size
982 for each year and location: our ability to estimate allele frequencies or detect subtle changes in
983 allele frequencies across time or space is limited. Sampling strategies that incorporate more
984 individuals, such as pooled sequencing (Bergland et al. 2014; Kapun et al. 2021; Machado et
985 al. 2021; Nunez et al. 2024), will be required to detect these more subtle changes, if they
986 occur, and to understand how they may contribute to rapid adaptation to new environments.
987 The recurrent nature of *Z. indianus* colonization may also offer insight towards the predictability
988 of rapid evolution of invasive species.
989
990 **Data Availability**
991
992 New individual sequencing data has been deposited in the SRA under project number #
993 PRJNA991922. RNA sequencing from larval and pupal samples, and larval Hi-C data used for
994 scaffolding are deposited under the same project number. The genome sequence has been
995 deposited at DDBJ/ENA/GenBank under the accession JAUIZU000000000. The metadata for
996 all sequencing samples (including date and location of collection); the annotation information
997 for transcripts, proteins and repeats; and VCFs of SNPs and structural variants have been
998 deposited to Dryad: https://doi.org/10.5061/dryad.q2bvq83v3. All code to reproduce analyses
999 has been deposited to Zenodo via Dryad. All code for analysis is also available at:
1000 https://github.com/ericksonp/Z.indianus_individual_sequencing/tree/main
1001
1002 Temporary reviewer dryad link:
1003 http://datadryad.org/stash/share/6td1mtLMrbgLL6IgyaEtpmqK4cigV0Vl2Hhqw9Aspvo
1004
1005 **Acknowledgments**

The authors acknowledge The University of Richmond's High Performance Computer (https://data.richmond.edu/About-HPC-at-UR/index.html) for providing computational resources that contributed to the results reported herein. We particularly thank George Flanagin for technical support. Preliminary analyses were conducted using resources provided by Research Computing at The University of Virginia (https://rc.virginia.edu). We thank the owners and managers of Carter Mountain Orchard and Hanover Peach Orchard for graciously allowing us to collect flies on their properties. We thank Melinda Yang for helpful suggestions on demographic analyses.

Funding

This work was funded by award 61-1673 from the Jane Coffin Childs Memorial Fund for Medical Research (to PAE), NIH NIGMS award R15GM146208 (to PAE), NSF BIO-DEB (EP) award 2145688 (to AOB), NIH NIGMS award R35GM119686 (to AOB), and startup funds from the University of Richmond to PAE.

Author contributions

PAE, AB, AOB: conceptualization; PAE, AOB: funding; PAE, AG: investigation; PAE, AB, NP: resources; PAE, AS: formal analysis, PAE: methodology, visualization, writing-original draft; PAE, AOB: writing-reviewing and editing

References

Alexander DH, Lange K. 2011. Enhancements to the ADMIXTURE algorithm for individual ancestry estimation. BMC Bioinformatics. 12(1):246. doi:10.1186/1471-2105-12-246. [accessed 2021 Jan 26]. https://doi.org/10.1186/1471-2105-12-246.

Allori Stazzonelli E, Funes CF, Corral Gonzalez MN, Gibilisco SM, Kirschbaum DS. 2023. Population fluctuation and infestation levels of Zaprionus indianus Gupta (Diptera: Drosophilidae) in berry crops of northwestern Argentina | International Society for Horticultural Science. Acta Horticultura.(1381). doi:10.17660/ActaHortic.2023.1381.19. [accessed 2024 Jun 19]. http://www.actahort.org/books/1381/1381_19.htm.

Altizer S, Ostfeld RS, Johnson PTJ, Kutz S, Harvell CD. 2013. Climate Change and Infectious Diseases: From Evidence to a Predictive Framework. Science. 341(6145):514–519. doi:10.1126/science.1239401.

Ananina G, Rohde C, David JR, Valente VLS, Klaczko LB. 2007. Inversion polymorphism and a new polytene chromosome map of Zaprionus indianus Gupta (1970) (Diptera: Drosophilidae). Genetica. 131(2):117–125. doi:10.1007/s10709-006-9121-6.

Animal and Plant Health Inspection Service. U.S. Regulated Plant Pest Table. [accessed 2025 Jun 9]. https://www.aphis.usda.gov/plant-imports/regulated-pest-list.

Araripe LO, Klaczko LB, Moreteau B, David JR. 2004. Male sterility thresholds in a tropical cosmopolitan drosophilid, Zaprionus indianus. Journal of Thermal Biology. 29(2):73–80. doi:10.1016/j.jtherbio.2003.11.006. [accessed 2019 Sep 5]. http://www.sciencedirect.com/science/article/pii/S0306456503000950.

Arredondo TM, Marchini GL, Cruzan MB. 2018. Evidence for human-mediated range expansion and gene flow in an invasive grass. Proceedings of the Royal Society B: Biological Sciences. 285(1882):20181125. doi:10.1098/rspb.2018.1125. [accessed 2024 Sep 5]. https://royalsocietypublishing.org/doi/full/10.1098/rspb.2018.1125.

Atsawawaranunt K, Ewart KM, Major RE, Johnson RN, Santure AW, Whibley A. 2023. Tracing the introduction of the invasive common myna using population genomics. Heredity. 131(1):56–67. doi:10.1038/s41437-023-00621-w. [accessed 2024 Jun 17]. https://www.nature.com/articles/s41437-023-00621-w.

Avalos A, Pan H, Li C, Acevedo-Gonzalez JP, Rendon G, Fields CJ, Brown PJ, Giray T, Robinson GE, Hudson ME, et al. 2017. A soft selective sweep during rapid evolution of gentle behaviour in an Africanized honeybee. Nat Commun. 8(1):1550. doi:10.1038/s41467-017-01800-0. [accessed 2024 Jun 25]. https://www.nature.com/articles/s41467-017-01800-0.

Bao Z, Eddy SR. 2002. Automated De Novo Identification of Repeat Sequence Families in Sequenced Genomes. Genome Res. 12(8):1269–1276. doi:10.1101/gr.88502. [accessed 2024 Feb 8]. https://genome.cshlp.org/content/12/8/1269.

Barrett CF, Corbett CW, Thixton-Nolan HL. 2023. A lack of population structure characterizes the invasive Lonicera japonica in West Virginia and across eastern North America1,2. tbot.

150(3):455–466. doi:10.3159/TORREY-D-23-00007.1. [accessed 2024 Jun 21]. https://bioone.org/journals/the-journal-of-the-torrey-botanical-society/volume-150/issue-3/TORREY-D-23-00007.1/A-lack-of-population-structure-characterizes-the-invasive-Lonicera-japonica/10.3159/TORREY-D-23-00007.1.full.

Barrett RDH, Laurent S, Mallarino R, Pfeifer SP, Xu CCY, Foll M, Wakamatsu K, Duke-Cohan JS, Jensen JD, Hoekstra HE. 2019. Linking a mutation to survival in wild mice. Science. 363(6426):499–504. doi:10.1126/science.aav3824.

Barrett SCH. 2015. Foundations of invasion genetics: the Baker and Stebbins legacy. Molecular Ecology. 24(9):1927–1941. doi:10.1111/mec.13014. [accessed 2019 Aug 29]. https://onlinelibrary.wiley.com/doi/abs/10.1111/mec.13014.

Battlay P, Leblanc PB, Green L, Garud NR, Schmidt JM, Fournier-Level A, Robin C. 2018. Structural Variants and Selective Sweep Foci Contribute to Insecticide Resistance in the Drosophila Genetic Reference Panel. G3 Genes|Genomes|Genetics. 8(11):3489–3497. doi:10.1534/g3.118.200619. [accessed 2021 Feb 9]. https://doi.org/10.1534/g3.118.200619.

Bellard C, Bertelsmeier C, Leadley P, Thuiller W, Courchamp F. 2012. Impacts of climate change on the future of biodiversity. Ecology Letters. 15(4):365–377. doi:https://doi.org/10.1111/j.1461-0248.2011.01736.x.

Bemmels JB, Mikkelsen EK, Haddrath O, Colbourne RM, Robertson HA, Weir JT. 2021. Demographic decline and lineage-specific adaptations characterize New Zealand kiwi. Proc Biol Sci. 288(1965):20212362. doi:10.1098/rspb.2021.2362.

Bergland AO, Behrman EL, O'Brien KR, Schmidt PS, Petrov DA. 2014. Genomic Evidence of Rapid and Stable Adaptive Oscillations over Seasonal Time Scales in Drosophila. PLoS Genet. 10(11):e1004775. doi:10.1371/journal.pgen.1004775. [accessed 2015 Nov 2]. http://dx.doi.org/10.1371/journal.pgen.1004775.

Bushnell B, Rood J, Singer E. 2017. BBMerge – Accurate paired shotgun read merging via overlap. PLOS ONE. 12(10):e0185056. doi:10.1371/journal.pone.0185056.

Cabanettes F, Klopp C. 2018. D-GENIES: dot plot large genomes in an interactive, efficient and simple way. PeerJ. 6:e4958. doi:10.7717/peerj.4958. [accessed 2024 Sep 18]. https://peerj.com/articles/4958.

Campos SRC, Rieger TT, Santos JF. 2007. Homology of polytene elements between Drosophila and Zaprionus determined by in situ hybridization in Zaprionus indianus. Genet Mol Res. 6(2):262–276.

Cantarel BL, Korf I, Robb SMC, Parra G, Ross E, Moore B, Holt C, Alvarado AS, Yandell M. 2008. MAKER: An easy-to-use annotation pipeline designed for emerging model organism genomes. Genome Res. 18(1):188–196. doi:10.1101/gr.6743907. [accessed 2024 Feb 8]. https://genome.cshlp.org/content/18/1/188.

Chan PP, Lowe TM. 2019. tRNAscan-SE: Searching for tRNA genes in genomic sequences. Methods Mol Biol. 1962:1–14. doi:10.1007/978-1-4939-9173-0_1. [accessed 2024 Feb 8]. https://www.ncbi.nlm.nih.gov/pmc/articles/PMC6768409/.

1108 Chang CC, Chow CC, Tellier LC, Vattikuti S, Purcell SM, Lee JJ. 2015. Second-generation
1109 PLINK: rising to the challenge of larger and richer datasets. Gigascience. 4:7.
1110 doi:10.1186/s13742-015-0047-8.

1111 Clements DR, Ditommaso A. 2011. Climate change and weed adaptation: can evolution of
1112 invasive plants lead to greater range expansion than forecasted? Weed Research. 51(3):227–
1113 240. doi:https://doi.org/10.1111/j.1365-3180.2011.00850.x.

1114 Comeault AA, Kautt AF, Matute DR. 2021. Genomic signatures of admixture and selection are
1115 shared among populations of Zaprionus indianus across the western hemisphere. Molecular
1116 Ecology. 30(23):6193–6210. doi:10.1111/mec.16066.

1117 Comeault AA, Wang J, Tittes S, Isbell K, Ingley S, Hurlbert AH, Matute DR. 2020. Genetic
1118 Diversity and Thermal Performance in Invasive and Native Populations of African Fig Flies.
1119 Molecular Biology and Evolution. 37(7):1893–1906. doi:10.1093/molbev/msaa050.

1120 Commar LS, Galego LG da C, Ceron CR, Carareto CMA. 2012. Taxonomic and evolutionary
1121 analysis of Zaprionus indianus and its colonization of Palearctic and Neotropical regions.
1122 Genet Mol Biol. 35(2):395–406. doi:10.1590/S1415-47572012000300003.

1123 Daborn P, Boundy S, Yen J, Pittendrigh B, ffrench-Constant R. 2001. DDT resistance in
1124 Drosophila correlates with Cyp6g1 over-expression and confers cross-resistance to the
1125 neonicotinoid imidacloprid. Mol Gen Genomics. 266(4):556–563. doi:10.1007/s004380100531.
1126 [accessed 2025 May 29]. https://doi.org/10.1007/s004380100531.

1127 Danecek P, Auton A, Abecasis G, Albers CA, Banks E, DePristo MA, Handsaker RE, Lunter G,
1128 Marth GT, Sherry ST, et al. 2011. The variant call format and VCFtools. Bioinformatics.
1129 27(15):2156–2158. doi:10.1093/bioinformatics/btr330. [accessed 2024 Sep 17].
1130 https://doi.org/10.1093/bioinformatics/btr330.

1131 Danecek P, Bonfield JK, Liddle J, Marshall J, Ohan V, Pollard MO, Whitwham A, Keane T,
1132 McCarthy SA, Davies RM, et al. 2021. Twelve years of SAMtools and BCFtools. Gigascience.
1133 10(2):giab008. doi:10.1093/gigascience/giab008.

1134 Díez-del-Molino D, Carmona-Catot G, Araguas R-M, Vidal O, Sanz N, García-Berthou E,
1135 García-Marín J-L. 2013. Gene Flow and Maintenance of Genetic Diversity in Invasive
1136 Mosquitofish (Gambusia holbrooki). PLOS ONE. 8(12):e82501.
1137 doi:10.1371/journal.pone.0082501. [accessed 2024 Sep 5].
1138 https://journals.plos.org/plosone/article?id=10.1371/journal.pone.0082501.

1139 Dobin A, Davis CA, Schlesinger F, Drenkow J, Zaleski C, Jha S, Batut P, Chaisson M,
1140 Gingeras TR. 2013. STAR: ultrafast universal RNA-seq aligner. Bioinformatics. 29(1):15–21.
1141 doi:10.1093/bioinformatics/bts635. [accessed 2024 Feb 8].
1142 https://www.ncbi.nlm.nih.gov/pmc/articles/PMC3530905/.

1143 Dowle M, Srinivasan A. 2019. data.table: Extension of `data.frame`. https://CRAN.R-
1144 project.org/package=data.table.

1145 Ellegren H. 2009. The different levels of genetic diversity in sex chromosomes and autosomes.
1146 Trends in Genetics. 25(6):278–284. doi:10.1016/j.tig.2009.04.005. [accessed 2024 Jun 24].
1147 https://www.sciencedirect.com/science/article/pii/S0168952509000900.

Ellstrand NC, Schierenbeck KA. 2000. Hybridization as a stimulus for the evolution of invasiveness in plants? Proceedings of the National Academy of Sciences. 97(13):7043–7050. doi:10.1073/pnas.97.13.7043. [accessed 2024 Jun 21]. https://www.pnas.org/doi/abs/10.1073/pnas.97.13.7043.

Erickson PA, Weller CA, Song DY, Bangerter AS, Schmidt P, Bergland AO. 2020. Unique genetic signatures of local adaptation over space and time for diapause, an ecologically relevant complex trait, in Drosophila melanogaster. PLOS Genetics. 16(11):e1009110. doi:10.1371/journal.pgen.1009110.

Estoup A, Ravigné V, Hufbauer R, Vitalis R, Gautier M, Facon B. 2016. Is There a Genetic Paradox of Biological Invasion? Annual Review of Ecology, Evolution, and Systematics. 47(Volume 47, 2016):51–72. doi:10.1146/annurev-ecolsys-121415-032116. [accessed 2025 Jun 11]. https://www.annualreviews.org/content/journals/10.1146/annurev-ecolsys-121415-032116.

Fang Z, Pyhäjärvi T, Weber AL, Dawe RK, Glaubitz JC, González J de JS, Ross-Ibarra C, Doebley J, Morrell PL, Ross-Ibarra J. 2012. Megabase-Scale Inversion Polymorphism in the Wild Ancestor of Maize. Genetics. 191(3):883–894. doi:10.1534/genetics.112.138578. [accessed 2024 Jun 24]. https://doi.org/10.1534/genetics.112.138578.

Felsenstein J. 2005. PHYLIP (Phylogeny Inference Package) version 3.6. https://phylipweb.github.io/phylip/.

Feron R, Waterhouse RM. 2022. Assessing species coverage and assembly quality of rapidly accumulating sequenced genomes. GigaScience. 11:giac006. doi:10.1093/gigascience/giac006. [accessed 2024 Jun 20]. https://doi.org/10.1093/gigascience/giac006.

Flynn JM, Hubley R, Goubert C, Rosen J, Clark AG, Feschotte C, Smit AF. 2020. RepeatModeler2 for automated genomic discovery of transposable element families. Proceedings of the National Academy of Sciences. 117(17):9451–9457. doi:10.1073/pnas.1921046117. [accessed 2024 Feb 8]. https://www.pnas.org/doi/full/10.1073/pnas.1921046117.

Fournier D, Aron S. 2021. Hybridization and invasiveness in social insects — The good, the bad and the hybrid. Current Opinion in Insect Science. 46:1–9. doi:10.1016/j.cois.2020.12.004. [accessed 2024 Jun 21]. https://www.sciencedirect.com/science/article/pii/S2214574521000018.

Friedline CJ, Faske TM, Lind BM, Hobson EM, Parry D, Dyer RJ, Johnson DM, Thompson LM, Grayson KL, Eckert AJ. 2019. Evolutionary genomics of gypsy moth populations sampled along a latitudinal gradient. Molecular Ecology. 0(0). doi:10.1111/mec.15069. [accessed 2019 Jun 6]. https://onlinelibrary.wiley.com/doi/abs/10.1111/mec.15069.

Galego LG da C, Carareto CMA. 2010. Variation at the Est3 locus and adaptability to organophosphorous compounds in Zaprionus indianus populations. Entomologia Experimentalis et Applicata. 134(1):97–105. doi:10.1111/j.1570-7458.2009.00941.x. [accessed 2025 May 29]. https://onlinelibrary.wiley.com/doi/abs/10.1111/j.1570-7458.2009.00941.x.

Galludo M, Canals J, Pineda-Cirera L, Esteve C, Rosselló M, Balanyà J, Arenas C, Mestres F. 2018. Climatic adaptation of chromosomal inversions in Drosophila subobscura. Genetica. 146(4):433–441. doi:10.1007/s10709-018-0035-x. [accessed 2024 Jun 20]. https://doi.org/10.1007/s10709-018-0035-x.

García-Escudero CA, Tsigenopoulos CS, Manousaki T, Tsakogiannis A, Marbà N, Vizzini S, Duarte CM, Apostolaki ET. 2023. Population genomics unveils the century-old invasion of the Seagrass Halophila stipulacea in the Mediterranean Sea. Mar Biol. 171(2):40. doi:10.1007/s00227-023-04361-7. [accessed 2024 Jun 17]. https://doi.org/10.1007/s00227-023-04361-7.

Garnier S. 2018. viridis: Default Color Maps from “matplotlib.” https://CRAN.R-project.org/package=viridis.

Garud NR, Messer PW, Buzbas EO, Petrov DA. 2015. Recent Selective Sweeps in North American Drosophila melanogaster Show Signatures of Soft Sweeps. PLOS Genetics. 11(2):e1005004. doi:10.1371/journal.pgen.1005004. [accessed 2021 Jan 21]. https://journals.plos.org/plosgenetics/article?id=10.1371/journal.pgen.1005004.

Gautier M. 2015. Genome-Wide Scan for Adaptive Divergence and Association with Population-Specific Covariates. Genetics. 201(4):1555–1579. doi:10.1534/genetics.115.181453. [accessed 2025 May 27]. https://doi.org/10.1534/genetics.115.181453.

Gautier M, Vitalis R. 2012. rehh: an R package to detect footprints of selection in genome-wide SNP data from haplotype structure. Bioinformatics. 28(8):1176–1177. doi:10.1093/bioinformatics/bts115.

Gleason JM, Roy PR, Everman ER, Gleason TC, Morgan TJ. 2019. Phenology of Drosophila species across a temperate growing season and implications for behavior. PLOS ONE. 14(5):e0216601. doi:10.1371/journal.pone.0216601.

Good BH, McDonald MJ, Barrick JE, Lenski RE, Desai MM. 2017. The dynamics of molecular evolution over 60,000 generations. Nature. 551(7678):45–50. doi:10.1038/nature24287.

Gupta JP. 1970. Description of a new species of Phorticella zaprionus (Drosophilidae) from India. Proceedings of the Indian National Science Academy. 36B(1):62–70.

Gupta JP, Kumar A. 1987. Cytogenetics of Zaprionus indianus Gupta (Diptera: Drosophilidae): Nucleolar organizer regions, mitotic and polytene chromosomes and inversion polymorphism. Genetica. 74(1):19–25. doi:10.1007/BF00055090. [accessed 2023 Jul 13]. https://doi.org/10.1007/BF00055090.

Hancock AM, Brachi B, Faure N, Horton MW, Jarymowycz LB, Sperone FG, Toomajian C, Roux F, Bergelson J. 2011. Adaptation to Climate Across the Arabidopsis thaliana Genome. Science. 334(6052):83–86. doi:10.1126/science.1209244.

Hannemann F, Bichet A, Ewen KM, Bernhardt R. 2007. Cytochrome P450 systems—biological variations of electron transport chains. Biochimica et Biophysica Acta (BBA) - General Subjects. 1770(3):330–344. doi:10.1016/j.bbagen.2006.07.017. [accessed 2025 May 29]. https://www.sciencedirect.com/science/article/pii/S0304416506002133.

He C, Liang J, Liu S, Zeng Y, Wang S, Wu Q, Xie W, Zhang Y. 2020. Molecular characterization of an NADPH cytochrome P450 reductase from *Bemisia tabaci* Q: Potential involvement in susceptibility to imidacloprid. Pesticide Biochemistry and Physiology. 162:29–35. doi:10.1016/j.pestbp.2019.07.018. [accessed 2025 May 29]. https://www.sciencedirect.com/science/article/pii/S0048357519304420.

Hoberg EP, Brooks DR. 2015. Evolution in action: climate change, biodiversity dynamics and emerging infectious disease. Philosophical Transactions of the Royal Society B: Biological Sciences. 370(1665):20130553. doi:10.1098/rstb.2013.0553.

Holle SG, Tran AK, Burkness EC, Ebbenga DN, Hutchison WD. 2018. First Detections of Zaprionus indianus (Diptera: Drosophilidae) in Minnesota. ents. 54(1):99–102. doi:10.18474/JES18-22.

Huang K, Andrew RL, Owens GL, Ostevik KL, Rieseberg LH. 2020. Multiple chromosomal inversions contribute to adaptive divergence of a dune sunflower ecotype. Molecular Ecology. 29(14):2535–2549. doi:10.1111/mec.15428. [accessed 2024 Jun 20]. https://onlinelibrary.wiley.com/doi/abs/10.1111/mec.15428.

Johnson MS, Gopalakrishnan S, Goyal J, Dillingham ME, Bakerlee CW, Humphrey PT, Jagdish T, Jerison ER, Kosheleva K, Lawrence KR, et al. 2021. Phenotypic and molecular evolution across 10,000 generations in laboratory budding yeast populations. Verstrepen KJ, Wittkopp PJ, Verstrepen KJ, Hodgins-Davis A, editors. eLife. 10:e63910. doi:10.7554/eLife.63910.

Jombart T. 2008. adegenet: a R package for the multivariate analysis of genetic markers. Bioinformatics. 24(11):1403–1405. doi:10.1093/bioinformatics/btn129. [accessed 2025 May 27]. https://doi.org/10.1093/bioinformatics/btn129.

Jombart T, Ahmed I. 2011. adegenet 1.3-1: new tools for the analysis of genome-wide SNP data. Bioinformatics. 27(21):3070–3071. doi:10.1093/bioinformatics/btr521. [accessed 2025 May 27]. https://doi.org/10.1093/bioinformatics/btr521.

Jones MR, Mills LS, Alves PC, Callahan CM, Alves JM, Lafferty DJR, Jiggins FM, Jensen JD, Melo-Ferreira J, Good JM. 2018. Adaptive introgression underlies polymorphic seasonal camouflage in snowshoe hares. Science. 360(6395):1355–1358. doi:10.1126/science.aar5273.

Joron M, Frezal L, Jones RT, Chamberlain NL, Lee SF, Haag CR, Whibley A, Becuwe M, Baxter SW, Ferguson L, et al. 2011. Chromosomal rearrangements maintain a polymorphic supergene controlling butterfly mimicry. Nature. 477(7363):203–206. doi:10.1038/nature10341. [accessed 2015 Sep 14]. http://www.nature.com/nature/journal/v477/n7363/full/nature10341.html.

Joshi NK, Biddinger DJ, Demchak K, Deppen A. 2014. First report of Zaprionus indianus (Diptera: Drosophilidae) in commercial fruits and vegetables in Pennsylvania. J Insect Sci. 14:259. doi:10.1093/jisesa/ieu121.

Kapun M, Nunez JCB, Bogaerts-Márquez M, Murga-Moreno J, Paris M, Outten J, Coronado-Zamora M, Tern C, Rota-Stabelli O, Guerreiro MPG, et al. 2021. Drosophila Evolution over Space and Time (DEST): A New Population Genomics Resource. Molecular Biology and

Evolution. 38(12):5782–5805. doi:10.1093/molbev/msab259. [accessed 2025 Jun 13]. https://doi.org/10.1093/molbev/msab259.

Keller O, Kollmar M, Stanke M, Waack S. 2011. A novel hybrid gene prediction method employing protein multiple sequence alignments. Bioinformatics. 27(6):757–763. doi:10.1093/bioinformatics/btr010. [accessed 2024 Feb 8]. https://doi.org/10.1093/bioinformatics/btr010.

Kim BY, Wang JR, Miller DE, Barmina O, Delaney E, Thompson A, Comeault AA, Peede D, D'Agostino ER, Pelaez J, et al. 2021. Highly contiguous assemblies of 101 drosophilid genomes. Coop G, Wittkopp PJ, Sackton TB, editors. eLife. 10:e66405. doi:10.7554/eLife.66405. [accessed 2023 Jul 13]. https://doi.org/10.7554/eLife.66405.

Koch JB, Dupuis JR, Jardeleza M-K, Ouedraogo N, Geib SM, Follett PA, Price DK. 2020. Population genomic and phenotype diversity of invasive Drosophila suzukii in Hawai'i. Biol Invasions. 22(5):1753–1770. doi:10.1007/s10530-020-02217-5. [accessed 2024 Jun 17]. https://doi.org/10.1007/s10530-020-02217-5.

Kohlmeier Pinar, Kohlmeier Philip. 2025. A non-overwintering urban population of the African fig fly (Diptera: Drosophilidae) impacts the reproductive output of locally adapted fruit flies. Florida Entomologist. 108(1). doi:10.1515/flaent-2024-0064. [accessed 2025 Mar 29]. https://www.degruyter.com/document/doi/10.1515/flaent-2024-0064/html?srsltid=AfmBOoqia32bki8F2DqWqVQeWln4SQ5boCJG7oVXUNkgD7qLXESk_noP.

Korf I. 2004. Gene finding in novel genomes. BMC Bioinformatics. 5(1):59. doi:10.1186/1471-2105-5-59. [accessed 2024 Feb 8]. https://doi.org/10.1186/1471-2105-5-59.

Korneliussen TS, Albrechtsen A, Nielsen R. 2014. ANGSD: Analysis of Next Generation Sequencing Data. BMC Bioinformatics. 15(1):356. doi:10.1186/s12859-014-0356-4. [accessed 2023 Jul 13]. https://doi.org/10.1186/s12859-014-0356-4.

Korunes KL, Samuk K. pixy: Unbiased estimation of nucleotide diversity and divergence in the presence of missing data. Molecular Ecology Resources. n/a(n/a). doi:https://doi.org/10.1111/1755-0998.13326. [accessed 2021 Feb 12]. https://onlinelibrary.wiley.com/doi/abs/10.1111/1755-0998.13326.

Kremmer L, David J, Borowiec N, Thaon M, Ris N, Poirie M, Gatti J-L. 2017. The African fig fly Zaprionus indianus: a new invasive pest in France? Bulletin of Insectology. 70(1):57–62.

Küpper C, Stocks M, Risse JE, dos Remedios N, Farrell LL, McRae SB, Morgan TC, Karlionova N, Pinchuk P, Verkuil YI, et al. 2016. A supergene determines highly divergent male reproductive morphs in the ruff. Nat Genet. 48(1):79–83. doi:10.1038/ng.3443. [accessed 2016 Mar 14]. http://www.nature.com/ng/journal/v48/n1/full/ng.3443.html.

Leão BFD, Tldon R. 2004. Newly invading species exploiting native host-plants: the case of the African Zaprionus indianus (Gupta) in the Brazilian Cerrado (Diptera, Drosophilidae). Annales de la Société entomologique de France (NS). 40(3–4):285–290. doi:10.1080/00379271.2004.10697427.

Lee YW, Fishman L, Kelly JK, Willis JH. 2016. A Segregating Inversion Generates Fitness Variation in Yellow Monkeyflower (Mimulus guttatus). Genetics. 202(4):1473–1484.

1308 doi:10.1534/genetics.115.183566. [accessed 2016 Apr 22].
1309 http://www.genetics.org/content/202/4/1473.

1310 Li H, Durbin R. 2009. Fast and accurate short read alignment with Burrows-Wheeler transform.
1311 Bioinformatics. 25(14):1754–1760. doi:10.1093/bioinformatics/btp324.

1312 Li H, Handsaker B, Wysoker A, Fennell T, Ruan J, Homer N, Marth G, Abecasis G, Durbin R,
1313 1000 Genome Project Data Processing Subgroup. 2009. The Sequence Alignment/Map format
1314 and SAMtools. Bioinformatics. 25(16):2078–2079. doi:10.1093/bioinformatics/btp352.
1315 [accessed 2022 Dec 9]. https://doi.org/10.1093/bioinformatics/btp352.

1316 Li H, Peng Y, Wang Y, Summerhays B, Shu X, Vasquez Y, Vansant H, Grenier C, Gonzalez N,
1317 Kansagra K, et al. 2023. Global patterns of genomic and phenotypic variation in the invasive
1318 harlequin ladybird. BMC Biol. 21(1):141. doi:10.1186/s12915-023-01638-7. [accessed 2024
1319 Jun 17]. https://doi.org/10.1186/s12915-023-01638-7.

1320 Li H, Ralph P. 2019. Local PCA Shows How the Effect of Population Structure Differs Along
1321 the Genome. Genetics. 211(1):289–304. doi:10.1534/genetics.118.301747. [accessed 2024
1322 May 14]. https://www.ncbi.nlm.nih.gov/pmc/articles/PMC6325702/.

1323 Linck E, Battey CJ. 2019. Minor allele frequency thresholds strongly affect population structure
1324 inference with genomic data sets. Molecular Ecology Resources. 19(3):639–647.
1325 doi:10.1111/1755-0998.12995. [accessed 2025 Jun 3].
1326 https://onlinelibrary.wiley.com/doi/abs/10.1111/1755-0998.12995.

1327 Linde K van der, Steck GJ, Hibbard K, Birdsley JS, Alonso LM, Houle D. 2006. FIRST
1328 RECORDS OF ZAPRIONUS INDIANUS (DIPTERA: DROSOPHILIDAE), A PEST SPECIES
1329 ON COMMERCIAL FRUITS FROM PANAMA AND THE UNITED STATES OF AMERICA. flen.
1330 89(3):402–404. doi:10.1653/0015-4040(2006)89[402:FROZID]2.0.CO;2.

1331 Lovell JT, MacQueen AH, Mamidi S, Bonnette J, Jenkins J, Napier JD, Sreedasyam A, Healey
1332 A, Session A, Shu S, et al. 2021 Jan 27. Genomic mechanisms of climate adaptation in
1333 polyploid bioenergy switchgrass. Nature.:1–7. doi:10.1038/s41586-020-03127-1.

1334 Lycett GJ, McLaughlin LA, Ranson H, Hemingway J, Kafatos FC, Loukeris TG, Paine MJI.
1335 2006. Anopheles gambiae P450 reductase is highly expressed in oenocytes and in vivo
1336 knockdown increases permethrin susceptibility. Insect Molecular Biology. 15(3):321–327.
1337 doi:10.1111/j.1365-2583.2006.00647.x. [accessed 2025 May 26].
1338 https://onlinelibrary.wiley.com/doi/abs/10.1111/j.1365-2583.2006.00647.x.

1339 Ma L, Cao L-J, Hoffmann AA, Gong Y-J, Chen J-C, Chen H-S, Wang X-B, Zeng A-P, Wei S-J,
1340 Zhou Z-S. 2020. Rapid and strong population genetic differentiation and genomic signatures of
1341 climatic adaptation in an invasive mealybug. Diversity and Distributions. 26(5):610–622.
1342 doi:https://doi.org/10.1111/ddi.13053. [accessed 2021 Jan 5].
1343 https://onlinelibrary.wiley.com/doi/abs/10.1111/ddi.13053.

1344 Ma L-J, Cao L-J, Chen J-C, Tang M-Q, Song W, Yang F-Y, Shen X-J, Ren Y-J, Yang Q, Li H,
1345 et al. 2024. Rapid and Repeated Climate Adaptation Involving Chromosome Inversions
1346 following Invasion of an Insect. Molecular Biology and Evolution. 41(3):msae044.

1347 doi:10.1093/molbev/msae044. [accessed 2024 Jun 17].
1348 https://doi.org/10.1093/molbev/msae044.

1349 Machado HE, Bergland AO, Taylor R, Tilk S, Behrman E, Dyer K, Fabian DK, Flatt T,
1350 González J, Karasov TL, et al. 2021. Broad geographic sampling reveals the shared basis and
1351 environmental correlates of seasonal adaptation in Drosophila. Nordborg M, Wittkopp PJ,
1352 Nordborg M, editors. eLife. 10:e67577. doi:10.7554/eLife.67577. [accessed 2024 Jun 20].
1353 https://doi.org/10.7554/eLife.67577.

1354 Manni M, Berkeley MR, Seppey M, Simão FA, Zdobnov EM. 2021. BUSCO Update: Novel and
1355 Streamlined Workflows along with Broader and Deeper Phylogenetic Coverage for Scoring of
1356 Eukaryotic, Prokaryotic, and Viral Genomes. Molecular Biology and Evolution. 38(10):4647–
1357 4654. doi:10.1093/molbev/msab199. [accessed 2024 Sep 19].
1358 https://doi.org/10.1093/molbev/msab199.

1359 Markow TA, Hanna G, Riesgo-Escovar JR, Tellez-Garcia AA, Richmond MP, Nazario-Yepiz
1360 NO, Laclette MRL, Carpinteyro-Ponce J, Pfeiler E. 2014. Population genetics and recent
1361 colonization history of the invasive drosophilid Zaprionus indianus in Mexico and Central
1362 America. Biol Invasions. 16(11):2427–2434. doi:10.1007/s10530-014-0674-5.

1363 da Mata RA, Tidon R, Côrtes LG, De Marco P, Diniz-Filho JAF. 2010. Invasive and flexible:
1364 niche shift in the drosophilid Zaprionus indianus (Insecta, Diptera). Biol Invasions. 12(5):1231–
1365 1241. doi:10.1007/s10530-009-9542-0.

1366 Matheson P, McGaughran A. 2022. Genomic data is missing for many highly invasive species,
1367 restricting our preparedness for escalating incursion rates. Sci Rep. 12(1):13987.
1368 doi:10.1038/s41598-022-17937-y. [accessed 2024 Jun 17].
1369 https://www.nature.com/articles/s41598-022-17937-y.

1370 McGaughran A, Dhami MK, Parvizi E, Vaughan AL, Gleeson DM, Hodgins KA, Rollins LA,
1371 Tepolt CK, Turner KG, Atsawawaranunt K, et al. 2024. Genomic Tools in Biological Invasions:
1372 Current State and Future Frontiers. Genome Biology and Evolution. 16(1):evad230.
1373 doi:10.1093/gbe/evad230. [accessed 2024 Jun 17]. https://doi.org/10.1093/gbe/evad230.

1374 McKenna A, Hanna M, Banks E, Sivachenko A, Cibulskis K, Kernytsky A, Garimella K,
1375 Altshuler D, Gabriel S, Daly M, et al. 2010. The Genome Analysis Toolkit: a MapReduce
1376 framework for analyzing next-generation DNA sequencing data. Genome Res. 20(9):1297–
1377 1303. doi:10.1101/gr.107524.110.

1378 Medley KA, Jenkins DG, Hoffman EA. 2015. Human-aided and natural dispersal drive gene
1379 flow across the range of an invasive mosquito. Molecular Ecology. 24(2):284–295.
1380 doi:10.1111/mec.12925. [accessed 2024 Sep 5].
1381 https://onlinelibrary.wiley.com/doi/abs/10.1111/mec.12925.

1382 Messer PW, Petrov DA. 2013. Population genomics of rapid adaptation by soft selective
1383 sweeps. Trends in Ecology & Evolution. 28(11):659–669. doi:10.1016/j.tree.2013.08.003.
1384 [accessed 2024 Jun 20]. https://www.cell.com/trends/ecology-evolution/abstract/S0169-
1385 5347(13)00207-3.

Microsoft, Weston S. 2017. foreach: Provides Foreach Looping Construct for R. https://CRAN.R-project.org/package=foreach.

Nava DE, Nascimento AM, Stein CP, Haddad ML, Bento JMS, Parra JRP. 2007. Biology, thermal requirements, and estimation of the number of generations of Zaprionus indianus (Diptera: Drosopholidae) for the main fig producing regions of Brazil. flen. 90(3):495–501. doi:10.1653/0015-4040(2007)90[495:BTRAEO]2.0.CO;2.

Nguyen Ba AN, Cvijović I, Rojas Echenique JI, Lawrence KR, Rego-Costa A, Liu X, Levy SF, Desai MM. 2019. High-resolution lineage tracking reveals travelling wave of adaptation in laboratory yeast. Nature. 575(7783):494–499. doi:10.1038/s41586-019-1749-3.

Nowling RJ, Manke KR, Emrich SJ. 2020. Detecting inversions with PCA in the presence of population structure. PLOS ONE. 15(10):e0240429. doi:10.1371/journal.pone.0240429. [accessed 2024 Jun 20]. https://journals.plos.org/plosone/article?id=10.1371/journal.pone.0240429.

Nunez JCB, Lenhart BA, Bangerter A, Murray CS, Mazzeo GR, Yu Y, Nystrom TL, Tern C, Erickson PA, Bergland AO. 2024. A cosmopolitan inversion facilitates seasonal adaptation in overwintering Drosophila. Genetics. 226(2):iyad207. doi:10.1093/genetics/iyad207. [accessed 2024 Jun 20]. https://doi.org/10.1093/genetics/iyad207.

Oerke E-C. 2006. Crop losses to pests. The Journal of Agricultural Science. 144(1):31–43. doi:10.1017/S0021859605005708.

Oliveira CM, Auad AM, Mendes SM, Frizzas MR. 2013. Economic impact of exotic insect pests in Brazilian agriculture. Journal of Applied Entomology. 137(1–2):1–15. doi:https://doi.org/10.1111/jen.12018.

de Oliveira Rios J, Costa SC, da Conceição Galego LG. 2024. Geographical and sex-specific effects of malathion insecticide selection in African fig fly Zaprionus indianus Gupta, 1970 (Diptera: Drosophilidae). Journal of Applied Entomology. 148(3):312–320. doi:10.1111/jen.13212. [accessed 2025 May 29]. https://onlinelibrary.wiley.com/doi/abs/10.1111/jen.13212.

Parchami-Araghi M, Gilasian E, Keyhanian A. 2015. Olive infestation with Zaprionus indianus Gupta (Dip.: Drosophilidae) in northern Iran: a new host record and threat to world olive production. Drosophila Information Service. 98:60–61.

Parvizi E, Dhami MK, Yan J, McGaughran A. 2023. Population genomic insights into invasion success in a polyphagous agricultural pest, Halyomorpha halys. Molecular Ecology. 32(1):138–151. doi:10.1111/mec.16740. [accessed 2024 Jun 17]. https://onlinelibrary.wiley.com/doi/abs/10.1111/mec.16740.

Patterson M, Marschall T, Pisanti N, van Iersel L, Stougie L, Klau GW, Schönhuth A. 2015. WhatsHap: Weighted Haplotype Assembly for Future-Generation Sequencing Reads. J Comput Biol. 22(6):498–509. doi:10.1089/cmb.2014.0157.

Patton AH, Margres MJ, Stahlke AR, Hendricks S, Lewallen K, Hamede RK, Ruiz-Aravena M, Ryder O, McCallum HI, Jones ME, et al. 2019. Contemporary Demographic Reconstruction Methods Are Robust to Genome Assembly Quality: A Case Study in Tasmanian Devils.

Molecular Biology and Evolution. 36(12):2906–2921. doi:10.1093/molbev/msz191. [accessed 2021 Jan 13]. https://doi.org/10.1093/molbev/msz191.

Pedersen BS, Layer R, Quinlan AR. 2020. smoove: structural-variant calling and genotyping with existing tools.

Pélissié B, Chen YH, Cohen ZP, Crossley MS, Hawthorne DJ, Izzo V, Schoville SD. 2022. Genome Resequencing Reveals Rapid, Repeated Evolution in the Colorado Potato Beetle. Molecular Biology and Evolution. 39(2):msac016. doi:10.1093/molbev/msac016. [accessed 2024 Jun 17]. https://doi.org/10.1093/molbev/msac016.

Pfeiffer DG, Shrader ME, Wahls JCE, Willbrand BN, Sandum I, van der Linde K, Laub CA, Mays RS, Day ER. 2019. African Fig Fly (Diptera: Drosophilidae): Biology, Expansion of Geographic Range, and Its Potential Status as a Soft Fruit Pest. J Integr Pest Manag. 10(1). doi:10.1093/jipm/pmz018. [accessed 2019 Aug 15]. https://academic.oup.com/jipm/article/10/1/20/5514212.

Pickrell JK, Pritchard JK. 2012. Inference of Population Splits and Mixtures from Genome-Wide Allele Frequency Data. PLOS Genetics. 8(11):e1002967. doi:10.1371/journal.pgen.1002967. [accessed 2025 May 29]. https://journals.plos.org/plosgenetics/article?id=10.1371/journal.pgen.1002967.

Picq S, Wu Y, Martemyanov VV, Pouliot E, Pfister SE, Hamelin R, Cusson M. 2023. Range-wide population genomics of the spongy moth, Lymantria dispar (Erebidae): Implications for biosurveillance, subspecies classification and phylogeography of a destructive moth. Evolutionary Applications. 16(3):638–656. doi:10.1111/eva.13522. [accessed 2024 Jun 20]. https://onlinelibrary.wiley.com/doi/abs/10.1111/eva.13522.

Platts PJ, Mason SC, Palmer G, Hill JK, Oliver TH, Powney GD, Fox R, Thomas CD. 2019. Habitat availability explains variation in climate-driven range shifts across multiple taxonomic groups. Scientific Reports. 9(1):15039. doi:10.1038/s41598-019-51582-2.

Price AL, Jones NC, Pevzner PA. 2005. De novo identification of repeat families in large genomes. Bioinformatics. 21(suppl_1):i351–i358. doi:10.1093/bioinformatics/bti1018. [accessed 2024 Feb 8]. https://doi.org/10.1093/bioinformatics/bti1018.

Purcell S, Neale B, Todd-Brown K, Thomas L, Ferreira MAR, Bender D, Maller J, Sklar P, de Bakker PIW, Daly MJ, et al. 2007. PLINK: a tool set for whole-genome association and population-based linkage analyses. Am J Hum Genet. 81(3):559–575. doi:10.1086/519795.

Putnam NH, O'Connell BL, Stites JC, Rice BJ, Blanchette M, Calef R, Troll CJ, Fields A, Hartley PD, Sugnet CW, et al. 2016. Chromosome-scale shotgun assembly using an in vitro method for long-range linkage. Genome Res. 26(3):342–350. doi:10.1101/gr.193474.115. [accessed 2023 Jul 13]. https://www.ncbi.nlm.nih.gov/pmc/articles/PMC4772016/.

R Core Team. R: A language and environment for statistical computing. http://www.R-project.org/.

Rakes LM, Delamont M, Cole C, Yates JA, Blevins LJ, Hassan FN, Bergland AO, Erickson PA. 2023. A small survey of introduced Zaprionus indianus (Diptera: Drosophilidae) in orchards of

1465 the eastern United States. Journal of Insect Science. 23(5):21. doi:10.1093/jisesa/iead092.
1466 [accessed 2024 Feb 8]. https://doi.org/10.1093/jisesa/iead092.

1467 Renkema JM, Iglesias LE, Bonneau P, Liburd OE. 2018. Trapping system comparisons for and
1468 factors affecting populations of Drosophila suzukii and Zaprionus indianus in winter-grown
1469 strawberry. Pest Management Science. 74(9):2076–2088. doi:10.1002/ps.4904. [accessed
1470 2025 Mar 29]. https://onlinelibrary.wiley.com/doi/abs/10.1002/ps.4904.

1471 Renkema JM, Miller M, Fraser H, Légaré J-P, Hallett RH. 2013. First records of *Zaprionus*
1472 *indianus* Gupta (Diptera: Drosophilidae) from commercial fruit fields in Ontario and Quebec,
1473 Canada. The Journal of the Entomological Society of Ontario. 144. [accessed 2021 Jan 25].
1474 https://journal.lib.uoguelph.ca/index.php/eso/article/view/3745.

1475 Ricciardi A. 2007. Are modern biological invasions an unprecedented form of global change?
1476 Conserv Biol. 21(2):329–336. doi:10.1111/j.1523-1739.2006.00615.x.

1477 Roman G, Meller V, Wu KH, Davis RL. 1998. The opt1 gene ofDrosophila melanogaster
1478 encodes a proton-dependent dipeptide transporter. American Journal of Physiology-Cell
1479 Physiology. 275(3):C857–C869. doi:10.1152/ajpcell.1998.275.3.C857. [accessed 2024 Sep 4].
1480 https://journals.physiology.org/doi/full/10.1152/ajpcell.1998.275.3.C857.

1481 Roque F, Matavelli C, Lopes PHS, Machida WS, Von Zuben CJ, Tidon R. 2017. Brazilian Fig
1482 Plantations Are Dominated by Widely Distributed Drosophilid Species (Diptera: Drosophilidae).
1483 Annals of the Entomological Society of America. 110(6):521–527. doi:10.1093/aesa/sax044.

1484 Sabeti PC, Reich DE, Higgins JM, Levine HZP, Richter DJ, Schaffner SF, Gabriel SB, Platko
1485 JV, Patterson NJ, McDonald GJ, et al. 2002. Detecting recent positive selection in the human
1486 genome from haplotype structure. Nature. 419(6909):832–837. doi:10.1038/nature01140.
1487 [accessed 2025 May 28]. https://www.nature.com/articles/nature01140.

1488 Sabeti PC, Varilly P, Fry B, Lohmueller J, Hostetter E, Cotsapas C, Xie X, Byrne EH, McCarroll
1489 SA, Gaudet R, et al. 2007. Genome-wide detection and characterization of positive selection in
1490 human populations. Nature. 449(7164):913–918. doi:10.1038/nature06250. [accessed 2021
1491 Feb 8]. https://www.ncbi.nlm.nih.gov/pmc/articles/PMC2687721/.

1492 Sardain A, Sardain E, Leung B. 2019. Global forecasts of shipping traffic and biological
1493 invasions to 2050. Nature Sustainability. 2(4):274–282. doi:10.1038/s41893-019-0245-y.

1494 Schluter D, Marchinko KB, Arnegard ME, Zhang H, Brady SD, Jones FC, Bell MA, Kingsley
1495 DM. 2021. Fitness maps to a large-effect locus in introduced stickleback populations. PNAS.
1496 118(3). doi:10.1073/pnas.1914889118. [accessed 2021 Jan 26].
1497 https://www.pnas.org/content/118/3/e1914889118.

1498 Schmidt JM, Good RT, Appleton B, Sherrard J, Raymant GC, Bogwitz MR, Martin J, Daborn
1499 PJ, Goddard ME, Batterham P, et al. 2010. Copy Number Variation and Transposable
1500 Elements Feature in Recent, Ongoing Adaptation at the Cyp6g1 Locus. PLOS Genetics.
1501 6(6):e1000998. doi:10.1371/journal.pgen.1000998. [accessed 2025 May 27].
1502 https://journals.plos.org/plosgenetics/article?id=10.1371/journal.pgen.1000998.

1503 Scott JG, Liu N, Wen Z. 1998. Insect cytochromes P450: diversity, insecticide resistance and
1504 tolerance to plant toxins1. Comparative Biochemistry and Physiology Part C: Pharmacology,

1505 Toxicology and Endocrinology. 121(1):147–155. doi:10.1016/S0742-8413(98)10035-X.
1506 [accessed 2025 May 29].
1507 https://www.sciencedirect.com/science/article/pii/S074284139810035X.

1508 Seebens H, Blackburn TM, Dyer EE, Genovesi P, Hulme PE, Jeschke JM, Pagad S, Pyšek P,
1509 Winter M, Arianoutsou M, et al. 2017. No saturation in the accumulation of alien species
1510 worldwide. Nature Communications. 8(1):14435. doi:10.1038/ncomms14435.

1511 Seebens H, Essl F, Dawson W, Fuentes N, Moser D, Pergl J, Pyšek P, Kleunen M van, Weber
1512 E, Winter M, et al. 2015. Global trade will accelerate plant invasions in emerging economies
1513 under climate change. Global Change Biology. 21(11):4128–4140.
1514 doi:https://doi.org/10.1111/gcb.13021.

1515 Shi L, Li W, Dong Y, Shi Y, Zhou Y, Liao X. 2021. NADPH-cytochrome P450 reductase
1516 potentially involved in indoxacarb resistance in *Spodoptera litura*. Pesticide Biochemistry and
1517 Physiology. 173:104775. doi:10.1016/j.pestbp.2021.104775. [accessed 2025 May 29].
1518 https://www.sciencedirect.com/science/article/pii/S0048357521000067.

1519 Siddiqui JA, Fan R, Naz H, Bamisile BS, Hafeez M, Ghani MI, Wei Y, Xu Y, Chen X. 2023.
1520 Insights into insecticide-resistance mechanisms in invasive species: Challenges and control
1521 strategies. Front Physiol. 13. doi:10.3389/fphys.2022.1112278. [accessed 2025 Jun 4].
1522 https://www.frontiersin.org/journals/physiology/articles/10.3389/fphys.2022.1112278/full.

1523 da Silva VH, Laine VN, Bosse M, Spurgin LG, Derks MFL, van Oers K, Dibbits B, Slate J,
1524 Crooijmans RPMA, Visser ME, et al. 2019. The Genomic Complexity of a Large Inversion in
1525 Great Tits. Genome Biology and Evolution. 11(7):1870–1881. doi:10.1093/gbe/evz106.
1526 [accessed 2024 Jun 24]. https://doi.org/10.1093/gbe/evz106.

1527 Simão FA, Waterhouse RM, Ioannidis P, Kriventseva EV, Zdobnov EM. 2015. BUSCO:
1528 assessing genome assembly and annotation completeness with single-copy orthologs.
1529 Bioinformatics. 31(19):3210–3212. doi:10.1093/bioinformatics/btv351. [accessed 2023 Jul 13].
1530 https://doi.org/10.1093/bioinformatics/btv351.

1531 Smit A, Hubley R, Green P. 2015. RepeatMasker Open-4.0. http://www.repeatmasker.org.

1532 Soudi S, Crepeau M, Collier TC, Lee Y, Cornel AJ, Lanzaro GC. 2023. Genomic signatures of
1533 local adaptation in recent invasive Aedes aegypti populations in California. BMC Genomics.
1534 24(1):311. doi:10.1186/s12864-023-09402-5. [accessed 2024 Jun 17].
1535 https://doi.org/10.1186/s12864-023-09402-5.

1536 Steenwyk JL, Rokas A. 2021. ggpubfigs: Colorblind-Friendly Color Palettes and ggplot2
1537 Graphic System Extensions for Publication-Quality Scientific Figures. Microbiology Resource
1538 Announcements. 10(44):10.1128/mra.00871-21. doi:10.1128/mra.00871-21. [accessed 2023
1539 Jul 13]. https://journals.asm.org/doi/10.1128/MRA.00871-21.

1540 Stern DB, Lee CE. 2020. Evolutionary origins of genomic adaptations in an invasive copepod.
1541 Nat Ecol Evol. 4(8):1084–1094. doi:10.1038/s41559-020-1201-y. [accessed 2024 Jun 18].
1542 https://www.nature.com/articles/s41559-020-1201-y.

1543 Stuart KC, Cardilini APA, Cassey P, Richardson MF, Sherwin WB, Rollins LA, Sherman CDH.
1544 2021. Signatures of selection in a recent invasion reveal adaptive divergence in a highly vagile

1545 invasive species. Molecular Ecology. 30(6):1419–1434. doi:https://doi.org/10.1111/mec.15601.
1546 [accessed 2021 Jan 5]. https://onlinelibrary.wiley.com/doi/abs/10.1111/mec.15601.

1547 Sutherst RW, Constable F, Finlay KJ, Harrington R, Luck J, Zalucki MP. 2011. Adapting to
1548 crop pest and pathogen risks under a changing climate. WIREs Climate Change. 2(2):220–
1549 237. doi:https://doi.org/10.1002/wcc.102.

1550 Suvorov A, Kim BY, Wang J, Armstrong EE, Peede D, D'Agostino ERR, Price DK, Waddell PJ,
1551 Lang M, Courtier-Orgogozo V, et al. 2022. Widespread introgression across a phylogeny of
1552 155 *Drosophila* genomes. Current Biology. 32(1):111-123.e5. doi:10.1016/j.cub.2021.10.052.
1553 [accessed 2024 Jun 21].
1554 https://www.sciencedirect.com/science/article/pii/S0960982221014962.

1555 Tait G, Mermer S, Stockton D, Lee J, Avosani S, Abrieux A, Anfora G, Beers E, Biondi A,
1556 Burrack H, et al. 2021. Drosophila suzukii (Diptera: Drosophilidae): A Decade of Research
1557 Towards a Sustainable Integrated Pest Management Program. Journal of Economic
1558 Entomology. 114(5):1950–1974. doi:10.1093/jee/toab158. [accessed 2025 Jun 9].
1559 https://doi.org/10.1093/jee/toab158.

1560 Tepolt CK, Grosholz ED, de Rivera CE, Ruiz GM. 2022. Balanced polymorphism fuels rapid
1561 selection in an invasive crab despite high gene flow and low genetic diversity. Molecular
1562 Ecology. 31(1):55–69. doi:10.1111/mec.16143. [accessed 2024 Jun 17].
1563 https://onlinelibrary.wiley.com/doi/abs/10.1111/mec.16143.

1564 Tepolt CK, Palumbi SR. 2020. Rapid Adaptation to Temperature via a Potential Genomic
1565 Island of Divergence in the Invasive Green Crab, Carcinus maenas. Front Ecol Evol. 8.
1566 doi:10.3389/fevo.2020.580701. [accessed 2024 Jun 20].
1567 https://www.frontiersin.org/articles/10.3389/fevo.2020.580701.

1568 Terhorst J, Kamm JA, Song YS. 2017. Robust and scalable inference of population history
1569 from hundreds of unphased whole-genomes. Nat Genet. 49(2):303–309. doi:10.1038/ng.3748.
1570 [accessed 2023 Jul 13]. https://www.ncbi.nlm.nih.gov/pmc/articles/PMC5470542/.

1571 Thompson MJ, Jiggins CD. 2014. Supergenes and their role in evolution. Heredity. 113(1):1–8.
1572 doi:10.1038/hdy.2014.20. [accessed 2015 Aug 11].
1573 http://www.nature.com/hdy/journal/v113/n1/full/hdy201420a.html.

1574 Thornton T, Tang H, Hoffmann TJ, Ochs-Balcom HM, Caan BJ, Risch N. 2012. Estimating
1575 kinship in admixed populations. Am J Hum Genet. 91(1):122–138.
1576 doi:10.1016/j.ajhg.2012.05.024.

1577 Timmeren SV, Isaacs R. 2014. Drosophila suzukii in Michigan vineyards, and the first report of
1578 Zaprionus indianus from this region. Journal of Applied Entomology. 138(7):519–527.
1579 doi:https://doi.org/10.1111/jen.12113.

1580 Uller T, Leimu R. 2011. Founder events predict changes in genetic diversity during human-
1581 mediated range expansions. Global Change Biology. 17(11):3478–3485. doi:10.1111/j.1365-
1582 2486.2011.02509.x. [accessed 2024 Jun 21].
1583 https://onlinelibrary.wiley.com/doi/abs/10.1111/j.1365-2486.2011.02509.x.

Vilela C. 1999. Is Zaprionus indianus Gupta, 1970 (Diptera, Drosophilidae) currently colonizing the Neotropical region? Drosophila Information Service. 82:37–39.

Voight BF, Kudaravalli S, Wen X, Pritchard JK. 2006. A Map of Recent Positive Selection in the Human Genome. PLOS Biology. 4(3):e72. doi:10.1371/journal.pbio.0040072. [accessed 2019 Apr 17]. https://journals.plos.org/plosbiology/article?id=10.1371/journal.pbio.0040072.

Wang K, Peng X, Zuo Y, Li Y, Chen M. 2016. Molecular Cloning, Expression Pattern and Polymorphisms of NADPH-Cytochrome P450 Reductase in the Bird Cherry-Oat Aphid Rhopalosiphum padi (L.). PLOS ONE. 11(4):e0154633. doi:10.1371/journal.pone.0154633. [accessed 2025 May 26]. https://journals.plos.org/plosone/article?id=10.1371/journal.pone.0154633.

Wang X, Chen X, Zhou T, Dai W, Zhang C. 2025. NADPH-cytochrome P450 reductase mediates resistance to neonicotinoid insecticides in *Bradysia odoriphaga*. Pesticide Biochemistry and Physiology. 211:106406. doi:10.1016/j.pestbp.2025.106406. [accessed 2025 May 23]. https://www.sciencedirect.com/science/article/pii/S0048357525001191.

Whiting JR, Paris JR, Zee MJ van der, Parsons PJ, Weigel D, Fraser BA. 2021. Drainage-structuring of ancestral variation and a common functional pathway shape limited genomic convergence in natural high- and low-predation guppies. PLOS Genetics. 17(5):e1009566. doi:10.1371/journal.pgen.1009566. [accessed 2025 May 27]. https://journals.plos.org/plosgenetics/article?id=10.1371/journal.pgen.1009566.

Wickham H. 2016. ggplot2: Elegant Graphics for Data Analysis.

Willbrand B, Pfeiffer D, Leblanc L, Yassin A. 2018. First Report of African Fig Fly, Zaprionus indianus Gupta (Diptera: Drosophilidae), on the Island of Maui, Hawaii, USA, in 2017 and Potential Impacts to the Hawaiian Entomofauna. Proceedings of the Hawaiian Entomological Society. 50:55–65.

Yassin A, Capy P, Madi-Ravazzi L, Ogereau D, David JR. 2008. DNA barcode discovers two cryptic species and two geographical radiations in the invasive drosophilid Zaprionus indianus. Molecular Ecology Resources. 8(3):491–501. doi:10.1111/j.1471-8286.2007.02020.x. [accessed 2019 Aug 15]. https://onlinelibrary.wiley.com/doi/abs/10.1111/j.1471-8286.2007.02020.x.

Yassin A, David J. 2010. Revision of the Afrotropical species of Zaprionus (Diptera, Drosophilidae), with descriptions of two new species and notes on the internal reproductive structures and immature stages. ZooKeys. 51:33–72. doi:10.3897/zookeys.51.380.

Zanuncio-Junior JS, Fornazier MJ, Andreazza F, Culik MP, Mendonça L de P, Oliveira EE, Martins D dos S, Fornazier ML, Costa H, Ventura JA. 2018. Spread of Two Invasive Flies (Diptera: Drosophilidae) Infesting Commercial Fruits in Southeastern Brazil. flen. 101(3):522–525. doi:10.1653/024.101.0328.

Zheng X, Levine D, Shen J, Gogarten SM, Laurie C, Weir BS. 2012. A high-performance computing toolset for relatedness and principal component analysis of SNP data. Bioinformatics. 28(24):3326–3328. doi:10.1093/bioinformatics/bts606.

1623